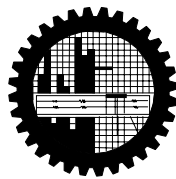


# Numerical Study of Magnetohydrodynamic Mixed Convection in a Partially Heated Rectangular Enclosure with Elliptic Block

by

Md. Imran Hossain  
Student No. 1017092505F  
Registration No. 1017092505, Session: October-2017


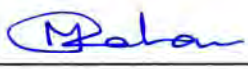
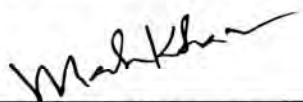

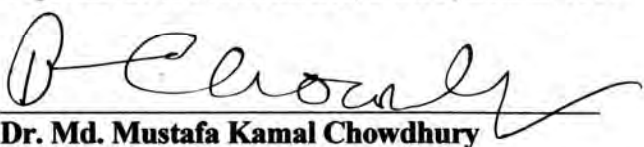
MASTER OF SCIENCE  
IN  
MATHEMATICS



Department of Mathematics  
BANGLADESH UNIVERSITY OF ENGINEERING AND  
TECHNOLOGY, DHAKA-1000  
August- 2019

The thesis entitled “Numerical Study of Magnetohydrodynamic Mixed Convection in a Partially Heated Rectangular Enclosure with Elliptic Block”, submitted by **Md. Imran Hossain**, Roll no: 1017092505F, Registration No. 1017092505, Session October 2017 has been accepted as satisfactory in partial fulfillment of the requirement for the degree of Master of Science in Mathematics on 04 August 2019.

## Board of Examiners

1.   
\_\_\_\_\_  
**Dr. Md. Abdul Maleque**  
Professor  
Department of Mathematics, BUET, Dhaka-1000  
Chairman  
(Supervisor)
2.   
\_\_\_\_\_  
**Head**  
Department of Mathematics  
BUET, Dhaka-1000  
Member  
(Ex-Officio)
3.   
\_\_\_\_\_  
**Dr. Md. Abdul Hakim Khan**  
Professor  
Department of Mathematics, BUET, Dhaka-1000  
Member
4.   
\_\_\_\_\_  
**Dr. Rehena Nasrin**  
Professor  
Department of Mathematics, BUET, Dhaka-1000  
Member
5.   
\_\_\_\_\_  
**Dr. Md. Mustafa Kamal Chowdhury**  
(Former) Professor  
Department of Mathematics, BUET, Dhaka-1000  
Member  
(External)

## **Candidate's Declaration**

I am hereby declaring that no portion of the work considered in this thesis has been submitted in support of an application for another degree or qualification of this or any other University or Institute of learning either in home or abroad.



---

**Md. Imran Hossain**

August 2019

## Certificate of Research

This is to certify that the work presented in this thesis is carried out by the author under the supervision of Dr. Md. Abdul Maleque, Professor, Department of Mathematics, Bangladesh University of Engineering & Technology, Dhaka.



---

**Dr. Md. Abdul Maleque**  
Professor  
Department of Mathematics  
BUET, Dhaka-1000.



---

**Md. Imran Hossain**  
Student No.1017092505  
Session: October 2017  
Status: Full-time

*Dedicated to my Parents*

## **Acknowledgement**

All praise is due to the Almighty ALLAH, the most merciful. I would like to affirm the notable recognizance of Almighty's continual mercy, because no work would have been possible to accomplish the goal without help Him. I am pleased to acknowledge with gratefulness to my supervisor Dr. Md. Abdul Maleque, Professor, Department of Mathematics, Bangladesh University of Engineering and Technology, for his guidance, constant support, intuitive suggestions and relentless encouragement which have been found very benevolent for the outcome of the research.

I would like to express my deepest gratitude to Dr. Md. Mustafizur Rahman, Professor, and Head, Department of Mathematics, Bangladesh University of Engineering and Technology, for his expert guidance and valuable suggestions in the course of being successful to reach the objectives of this dissertation. I would also like to express my sincere thanks and gratitude to Dr. Md. Abdul Hakim Khan, Professor, Department of Mathematics, BUET and Dr. Rehana Nasrin, Professor, Department of mathematics, BUET for many helpful discussions and suggestions during my study support that was crucial for the success of this work. I also express my gratitude to all my respectable teachers, Department of Mathematics, BUET, for their help and heartiest co-operation.

I am grateful to the external member of the Board of Examiners, Dr. Md. Mustafa Kamal Chowdhury, Former Professor, Department of Mathematics, BUET, for his valuable suggestions in improving the quality of the work.

I am also grateful to Mohammad Mokaddes Ali, Associate Professor, Department of Mathematics, Mawlana Bhashani Science and Technology University, Tangail, for his encouragement and helping mentality in all affairs especially in my research work.

Also I wish thanks to the staff of the Department of Mathematics, BUET, for their cooperation in this work.

Finally I express my devoted affection to all my family members specially my parents for co-operation to do this study.

## Abstract

Magnetohydrodynamic mixed convection fluid flow and heat transfer in a partially heated rectangular enclosure with elliptic block has been investigated numerically in this study. The left wall of the enclosure has been supposed to high temperature,  $T_h$  whereas the right wall has been maintained at low temperature,  $T_c$  while the remaining walls have been kept adiabatic. The top adiabatic wall has been kept lid-driven with constant velocity parallel to the positive x-direction. A uniform magnetic field of strength,  $B_0$  is applied parallel to the x-axis. The Physical problem has been presented mathematically by different sets of governing differential equations (such as mass, momentum and energy equations) along with the corresponding initial and boundary conditions. By using appropriate transformations, the governing equations along with the boundary conditions have been transformed into non-dimensional form, which have been then solved by employing a finite-element scheme based on the Galerkin method of weighted residuals.

Numerical results have been obtained for a wide range of dimensionless parameters such as Richardson number, Hartmann number, Prandtl number, Reynolds number and the physical parameter namely area of elliptical block. Also, these results have been presented graphically in the form of streamlines, isothermal contours, and average Nusselt number along the heated section of the vertical left wall at the three values of Richardson number ( $Ri$ ), varying from 0.1 to 10. This range of  $Ri$  have been selected on the basis of calculation covering pure forced convection, pure mixed convection and free convection dominated regimes. In mixed convection dominated region, the heat transfer decreases 4.74, 16.58, and 44.16% with increasing Hartmann number from  $Ha = 0$  to 10, 20, and 50, respectively. On the other hand, the heat transfer increases 51.34, 89.52, and 118.82% with increasing Reynolds number from  $Re = 50$  to 100, 150, and 200, respectively.

# Table of Contents

<u>Items</u>	<u>Page</u>
<b>Board of Examiners</b> .....	Error! Bookmark not defined.
<b>Candidate’s Declaration</b> .....	<b>ii</b>
<b>Certificate of Research</b> .....	<b>iii</b>
<b>Acknowledgement</b> .....	<b>vi</b>
<b>Abstract</b> .....	<b>vii</b>
Nomenclature .....	x
List of Tables.....	xii
List of Figures .....	xii
<b>Chapter 1</b> .....	<b>1</b>
Introduction .....	1
1.1 Magnetohydrodynamic.....	1
1.2 Heat Transfer Mechanism .....	2
1.2.1 Convection .....	3
1.2.2 Conduction .....	3
1.2.3 Radiation .....	4
1.2.4 Mixed convection heat transfer in enclosures.....	4
1.3 Dimensionless Parameter .....	5
1.3.1 Reynolds number .....	5
1.3.2 Prandtl number .....	6
1.3.3 Hartmann number .....	6
1.3.4 Richardson number .....	6
1.4 Literature Review .....	6
1.5 Motivation .....	10
1.6 Present Research .....	10
1.7 Objectives.....	11
1.8 Outline of the Thesis .....	12
<b>Chapter 2</b> .....	<b>13</b>
Computational Details.....	13
2.1 Advantages of Numerical Investigation.....	14



2.2 Components of a Numerical Solution Methods .....	14
2.2.1 Mathematical model.....	14
2.2.2 Discretization method .....	15
2.2.3 Numerical grid .....	15
2.2.4 Finite approximations .....	15
2.2.5 Solution method .....	15
2.3 Discretization Approaches .....	16
2.3.1 Finite element method.....	16
2.3.2 Grid generation .....	17
2.3.3 Finite element formulation and computational procedure .....	18
2.3.4 Algorithm .....	18
<b>Chapter 3 .....</b>	<b>20</b>
Mathematical Modeling .....	20
3.1 General .....	20
3.2 Physical Configuration.....	20
3.3 Mathematical Formulation .....	21
3.3.1 Governing equations .....	21
3.3.2 Boundary conditions .....	22
3.3.3 Dimensional analysis .....	23
3.3.4 Grid sensitivity test .....	24
3.3.5 Validation of the numerical scheme.....	26
<b>Chapter 4 .....</b>	<b>28</b>
Results and Discussion.....	28
4.1 Effect of Hartmann number .....	29
4.2 Effect of Reynolds number .....	35
4.3 Effect of Prandtl number.....	40
4.4 Effect of area of block.....	46
<b>Chapter 5 .....</b>	<b>52</b>
Conclusions .....	52
5.1 Summary of the Major Outcomes .....	52
5.2 Further Works .....	53
References .....	54

## Nomenclature

$B_0$	magnetic induction ( $Wb/m^2$ )
$c_p$	specific heat at constant pressure ( $J/kg.K$ )
$g$	gravitational acceleration ( $ms^{-2}$ )
$Gr$	Grashof number
$h$	convective heat transfer coefficient ( $W/m^2.K$ )
$H$	height of the enclosure ( $m$ )
$Ha$	Hartmann number
$k$	thermal conductivity of fluid ( $Wm^{-1}K^{-1}$ )
$L$	length of the enclosure ( $m$ )
$n$	dimensional distance either along $x$ or $y$ direction ( $m$ )
$N$	non-dimensional distance either along $X$ or $Y$ direction
$Nu_1$	local Nusselt number
$Nu$	Average Nusselt number
$p$	pressure
$P$	non-dimensional pressure
$Pr$	Prandtl number
$Re$	Reynolds number
$Ri$	Richardson number
$T$	dimensional fluid temperature ( $K$ )
$T_s$	dimensional solid temperature ( $K$ )
$\Delta T$	dimensional temperature difference ( $K$ )
$u$	velocity in $x$ -direction ( $m/s$ )
$U$	dimensionless horizontal velocity
$U_0$	lid velocity ( $m/s$ )
$v$	velocity in $y$ -direction ( $m/s$ )
$V$	dimensionless vertical velocity
$\bar{V}$	enclosure volume ( $m^3$ )
$x, y$	Cartesian coordinates ( $m$ )
$X, Y$	dimensionless Cartesian coordinates

## Greek symbols

$\alpha$	thermal diffusivity ( $m^2s^{-1}$ )
$\beta$	coefficient of thermal expansion ( $K^{-1}$ )
$\Delta\theta$	dimensionless temperature difference
$\mu$	dynamic viscosity of the fluid ( $m^2s^{-1}$ )
$\nu$	kinematic viscosity of the fluid ( $m^2s^{-1}$ )
$\rho$	density of the fluid ( $kgm^{-3}$ )
$\sigma$	fluid electrical conductivity ( $\Omega^{-1}.m^{-1}$ )

## **Subscripts**

<i>av</i>	average
<i>h</i>	heated wall
<i>l</i>	local

## **Abbreviation**

CBC	convective boundary conditions
CFD	computational fluid dynamics
FDM	finite difference method
FVM	finite volume method
FEM	finite element method

## List of Tables

3.1	Grid sensitivity check at $Re = 100$ , $Ri = 1.0$ , $Ha = 10$ and $Pr = 0.71$ .	25
4.1	Variation of the average Nusselt number with Hartmann number for different Richardson number.	33
4.2	Variation of the average Nusselt number with Reynolds number for different Richardson number.	39
4.3	Variation of the average Nusselt number with Prnadtl number for different Richardson number.	45
4.4	Variation of the average Nusselt number with area of block for different Richardson number.	50

## List of Figures

1.1	Heat Transfer Mechanisms	2
2.1	A typical FE discretization of a domain, Reddy & Gartling [38].	18
2.2	Flow chart of the computational procedure.	19
3.1	The schematic diagrams of partially heated lid-driven rectangular enclosure with an elliptical block.	21
3.2	Grid sensitivity test at $Ri = 1.0$ , $Re = 100$ , $Ha = 10$ and $Pr = 0.71$ .	26
3.3	Current mesh structure with 8313 numbers of nodes for present study.	26
3.4	Code validation for present research.	27
4.1	Effect of Hartmann number on Streamlines and Isotherms while $Ri = 0.1$ , $Re = 100$ , $Pr = 0.71$ .	30
4.2	Effect of Hartmann number on Streamlines and Isotherms while $Ri = 1$ , $Re = 100$ , $Pr = 0.71$ .	31
4.3	Effect of Hartmann number on Streamlines and Isotherms while $Ri = 10$ , $Re = 100$ , $Pr = 0.71$ .	32
4.4	Effect of Hartmann Number ( $Ha$ ) on average Nusselt number, while $Re = 100$ , $Pr = 0.71$ .	33
4.5	Effect of Reynolds number on Streamlines and Isotherms while $Ri = 0.1$ ,	36

	$Ha = 10, Pr = 0.71.$	
4.6	Effect of Reynolds number on Streamlines and Isotherms while $Ri = 1.0,$ $Ha = 10, Pr = 0.71.$	37
4.7	Effect of Reynolds number on Streamlines and Isotherms while $Ri = 10,$ $Ha = 10, Pr = 0.71.$	38
4.8	Effect of Reynolds Number ( $Re$ ) on average Nusselt number, while $Ha =$ $10, Pr = 0.71.$	39
4.9	Effect of Prandtl number on Streamlines and Isotherms while $Ri = 0.1, Ha$ $= 10, Re = 100.$	42
4.10	Effect of Prandtl number on Streamlines and Isotherms while $Ri = 1.0, Ha$ $= 10, Re = 100.$	43
4.11	Effect of Prandtl number on Streamlines and Isotherms while $Ri = 10, Ha$ $= 10, Re = 100.$	44
4.12	Effect of Prandtl Number ( $Pr$ ) on average Nusselt number, while $Re =$ $100, Ha = 10.$	45
4.13	Effect of Streamlines and Isotherms on different elliptical area at Richardson number $Ri = 0.1$ while $Re = 100, Ha = 10.0$ and $Pr = 0.71.$	47
4.14	Effect of Streamlines and Isotherms on different elliptical area at Richardson number $Ri = 0.1$ while $Re = 100, Ha = 10.0$ and $Pr = 0.71.$	48
4.15	Effect of Streamlines and Isotherms on different elliptical area at Richardson number $Ri = 0.1$ while $Re = 100, Ha = 10.0$ and $Pr = 0.71.$	49
4.16	Effect of area of block on average Nusselt number, while $Re = 100, Pr =$ $0.71$ and $Ha = 10.$	50

# Chapter 1

## Introduction

---

Fluid flow and heat transfer in an enclosure is an important development and a part of very rapid growth in contemporary movement of heat transfer research. Mixed convective heat transfer inside an enclosure in the presence of magnetic field is a recent branch of thermo-fluid Mechanics. Thermo-fluid is the combined study of heat transfer, fluid dynamics, thermodynamics and combustion.

The effect of mixed convection flow in rectangular enclosure has been studied by many researchers and it has been a very popular research topic for many years. Mixed convection flows are important in the context of many engineering applications for predicting the performance, designing of much equipment, machine parts like small microchips to large nuclear reactor. But things used in practical purpose are much more complicated in design and prediction of their performance using results from simple geometry cause huge error. For this complexity, in recent years, attention has been given to study hydrodynamic and thermal characteristics of complex geometry. Among those the enclosures incorporating solid bodies or partitions are given special attention due to their wide applications in computer hardware, heat exchangers, solar heat collector, some air conditioning equipment and furnaces etc. A study of the flow of electrically conducting fluid in presence of magnetic field is also important from the technical point of view and such types of problems have received much attention by many investigators.

### 1.1 Magnetohydrodynamic

Magnetohydrodynamic (MHD) is that branch of science, which deals with the flow of electrically conducting fluids in electric and magnetic fields. The motion of the conducting fluid across the magnetic field generates electric currents which change the magnetic field and the action of the magnetic field on these currents give rise to mechanical forces, which modify the fluid. However, MHD is usually regarded as a very contemporary subject. Probably the largest advance towards an understanding of such phenomena comes from the fields of astrophysics and geophysics. It has long

been assumed that most of the matter in the universe is in the plasma or highly ionized state and much of the basic knowledge in the area of electromagnetic fluid dynamics evolved from these studies. Moreover MHD explains certain natural phenomena. The motions of the sea induced magnetic field that perturb the earth's magnetic field. Alternatively the electromagnetic force due to the interaction of currents and earth's magnetic field propels ocean movements. The MHD was originally applied to astrophysical and geophysical problems, where it is still very important. Engineers employ MHD principles in the design of heat exchanger, pumps and flow meters, in space vehicle propulsion, control and re-entry in creating novel power generating systems and developing confinement schemes for controlled fusion. Other potential applications for MHD include electromagnets with fluid conductors, various energy conversion or storage devices, and magnetically controlled lubrication by conducting fluids etc. Detailed discussion of the Magnetohydrodynamic (MHD) can be found in Shercliff [34].

## 1.2 Heat Transfer Mechanism

Heat is a form of energy that can be transferred from one system to another as a result of temperature difference. A thermodynamic analysis is concerned with the amount of heat transfer as a system undergoes a process from one equilibrium state to another. The science that deals with the determination of the rates of such energy transfer is the heat transfer. The transfer of energy is always from the higher temperature medium to the lower temperature one and heat transfer stops when the two medium reach the same temperature.

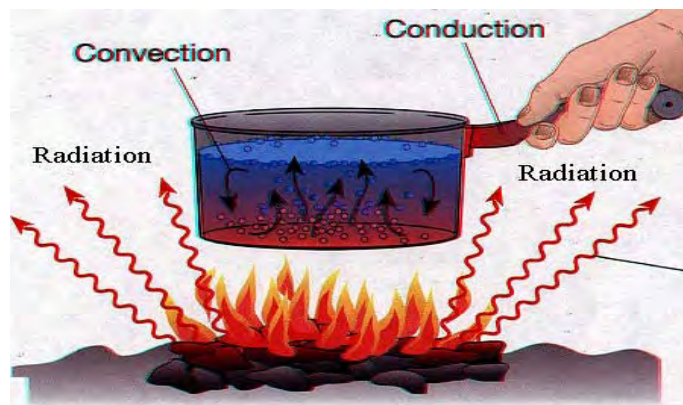


Figure 1.1: Heat transfer mechanism.

Heat can be transferred in three different mechanism or modes: conduction, convection, and radiation. All modes of heat transfer require the existence of temperature difference, and all modes are from the high temperature medium to a lower temperature one. In reality the combined effect of these three modes of heat transfers control temperature distribution in a medium. Details are found in Kakac and Yener [39]. Brief descriptions of convection, conduction, and radiation modes are given below:

### **1.2.1 Convection**

Convection is that mode of heat transfer where energy exchange occurs between the particles by convection current. It may be explained as; when fluid flows over a solid body or inside a channel while the temperatures of the fluid and solid surfaces are different, heat transfer between the fluid and solid surface takes place as consequences of the motion of the fluid relative to the surfaces.

The convective heat transfer bifurcates into two branches; the natural convection and forced convection. If the fluid is forced to flow over the surface by external means such as a fan, pump, or the wind, the convection is called forced convection. But the fluid motion caused by buoyancy forces that are induced by density difference due to the variation of temperature in the field is called natural (or free) convection. Buoyancy is due to the combined presence of the fluid density gradient and body force.

### **1.2.2 Conduction**

Conduction is the transfer of energy from the more energetic particles of a substance to the adjacent less energetic one as a result of interactions between the particles. Conduction can take place in solids, liquids, or gasses. The rate of heat conduction through a medium depends on the geometry of the medium, its thickness, and the material of the medium, as well as the temperature difference across the medium.



### **1.2.3 Radiation**

The energy emitted by matter in the form of electromagnetic waves as a result of the changes in the electronic configurations of the atoms or molecules is called radiation. The transfer of energy by radiation does not require the presence of a medium like as conduction and convection. Radiation occurs through a vacuum or any transparent medium. Thermal radiation is the direct result of random movements of atoms and molecules in matter. Movement of the charged protons and electrons results in the emission of electromagnetic radiation. All materials radiate thermal energy based on their temperature. The hotter an object, the more it will radiate. In fact, energy transfer by radiation is fastest (at the speed of light) and it suffers no attenuation in a vacuum. This is how the energy of the sun reaches the earth.

### **1.2.4 Mixed convection heat transfer in enclosures**

Mixed convection in enclosures is a topic of contemporary importance, because enclosures filled with fluid are central components in a long list of engineering and geophysical systems. The flow and heat transfer induced in an enclosure differs fundamentally from the external mixed convection boundary layer. Mixed convection in an enclosure, like the external mixed convection boundary layer that is caused by the heat transfer interaction between a single wall and a very large fluid reservoir is the result of the complex interaction between finite size fluid systems in thermal communication with all the walls that confine it. The complexity of this internal interaction is responsible for the diversity of flows that can exist inside enclosure.

The phenomenon of mixed convection in enclosures is varied by the geometry and the orientation of the enclosure. Judging by the potential engineering applications, the enclosure phenomena can loosely be organized into two classes:

1. Vented enclosure and
2. Lid-driven enclosure

In a vented enclosure, where the interaction between the external forced stream provided by the inlet and the buoyancy driven flows induced by the heat source leads to the possibility of complex flows. Therefore it is important to understand the fluid

flow and heat transfer characteristics of mixed convection in a vented enclosure. On the other hand, the fluid flow and heat transfer in a lid-driven enclosure where the flow is induced by a shear force resulting from the motion of a lid combined with the buoyancy force due to non-homogeneous temperature of the enclosure wall, provides another problem, studied extensively by researchers to understand the interaction between buoyancy and shearing forces in such flow situation. The interaction between buoyancy driven and shear driven flows inside a closed enclosure in a mixed convection regime is quite complex. Therefore it is also important to understand the fluid flow and heat transfer characteristics of mixed convection in a lid-driven enclosure.

### 1.3 Dimensionless Parameter

The dimensionless parameters can be considered as measures of the relative importance of certain aspects of the flow. Some dimensionless parameters related to the present study are discussed below:

#### 1.3.1 Reynolds number

The Reynolds number ( $Re$ ) is the ratio of the inertial forces to viscous forces within a fluid which is subjected to relative internal movement due to different fluid velocities, which is known as a boundary layer. The Reynolds number is defined as

$$Re = \frac{\rho u L}{\mu} = \frac{u L}{\nu}$$

where

- $\rho$  is the density of the fluid
  - $u$  is the velocity of the fluid with respect to the object.
  - $L$  is the characteristics length
  - $\mu$  is the dynamic viscosity
1. Laminar flow occurs at low Reynolds numbers, where viscous forces are dominant, and is characterized by smooth, constant fluid motion.
  2. Turbulent flow occurs at high Reynolds number and is dominated by inertial forces, which tend to produce chaotic eddies, vortices and other flow instabilities.

### 1.3.2 Prandtl number

The Prandtl number ( $Pr$ ) is a dimensionless number which is defined as the ratio of momentum diffusivity to thermal diffusivity. That is, the Prandtl number is given as

$$Pr = \frac{\nu}{\alpha} = \frac{\text{momentum diffusivity}}{\text{thermal diffusivity}} = \frac{c_p \mu}{k}$$

where  $k$  is thermal conductivity,  $c_p$  is the specific heat. The Prandtl numbers of fluids range from less than 0.01 for liquid metals to more than 100000 for heavy oils for water 1-10 and for gases  $Pr$  ranges are 0.7-1.0.

### 1.3.3 Hartmann number

Hartmann number ( $Ha$ ) is the ratio of electromagnetic force to the viscous force first introduced by Hartmann. It is frequently encountered in fluid flows through magnetic fields. It is defined by

$$Ha = BL \sqrt{\frac{\sigma}{\mu}}$$

where  $B$  is the magnetic field intensity,  $L$  is the characteristics length,  $\sigma$  is the electrical conductivity,  $\mu$  is the dynamic viscosity.

### 1.3.4 Richardson number

The Richardson number ( $Ri$ ) is the dimensionless number that expresses the ratio of the buoyancy term to the flow shear term. It is defined as

$$Ri = \frac{\text{buoyancy term}}{\text{flow shear term}} = \frac{g \left( \frac{\partial \rho}{\partial z} \right)}{\rho \left( \frac{\partial \rho}{\partial z} \right)^2}$$

Typically, the natural convection is negligible when  $Ri < 0.1$ , forced convection is negligible when  $Ri > 10$ , and mixed convection is dominant when  $0.1 < Ri < 10$ .

## 1.4 Literature Review

Mixed convection flows occur when both forced convection and natural convection dominate. The study of mixed convection in a lid-driven enclosure plays an important role in engineering, industries such as cooling of electronic devices,

furnaces, design of solar collectors, thermal design of building, air conditioning and drying technologies etc. Various researchers investigated the effects of mixed convective flows in cavities, channels by using analytical, experimental and numerical methods. Some important works are presented below.

Chowdhury and Alim [1] investigated MHD mixed convection flow within a square enclosure with triangular obstacle. They found that heat transfer rate is higher in absence of magnetic field and for higher Richardson number. Khudheyer [2] analyzed MHD mixed convection in double lid-driven differentially heated trapezoidal cavity. He considered different inclination angles at trapezoidal cavity. He found that in the mixed convection region, in the absence of magnetic field ( $Ha = 0$ ), the maximum heat transfer occurs at the trapezoidal cavity ( $\theta = 30^\circ$ ) and Nusselt number decreases with increasing Hartmann number ( $Ha$ ). Mixed convection in lid-driven cavity with inclined magnetic field is studied by Baker *et al.* [3]. They concluded that average Nusselt number ( $Nu$ ) increases by increasing the magnetic field angle. Parvin and Nasrin [4] performed the flow and heat transfer characteristics for MHD free convection in an enclosure with a heated obstacle. The summary of their investigation was that the diameter of the heated obstacle has a significant change on the flow and temperature fields. Also they found that average Nusselt number decreases with increasing Hartmann number.

Saha *et al.* [5] studied mixed convection heat transfer in a lid-driven cavity with wavy bottom surface. They found that Reynolds number, Grashof number and the number of undulations of the wavy surface have significant effect on the flow fields. Ismail *et al.* [6] studied mixed convection in a lid-driven square cavity with partial slip. They showed that the convection is declined due to critical values for the partial slip parameter. Sumon *et al.* [7] presented a numerical study of the effect of inclination angle on mixed convection in a lid-driven enclosure. They observed that heat transfer rate increases from the bottom wall due to internal heat absorption other than internal heat generation. Also they found that average Nusselt number over the base wall is to be more prominent at higher base wall inclination angles in all cases of heat generation.

A numerical simulation on MHD mixed convection in a lid-driven cavity with corner heaters is presented by Malleswaran and Sivasankaran [8]. They observed that the

heater length in the x-direction is more effective than that of in the y-direction on the heat transfer and on the flow pattern. Also they found that average Nusselt number ( $Nu$ ) is more on vertical heaters than on the horizontal heaters. The study Magneto-hydrodynamics (MHD) containing the influence of magnetic field on heat transfer and fluid flow within the cavity has received a considerable attention in recent years. The widespread practical applications of MHD convection in the sectors such as solar technologies, material manufacturing technology, electromagnetic casting, liquid-metal cooling of nuclear reactors and plasma confinement due to this reason. Nasrin [9] investigated mixed convection in a lid driven cavity with a sinusoidal wavy wall and a central heat conducting body. She considered a heat conducting square body located at the center of cavity. She observed that the influence of Hartmann number ( $Ha$ ) does not affect the thermal current activities. Convective heat transfer in a square cavity with a heat generating body of different aspect ratios is performed by Afolabi *et al.* [10]. They observed that heat transfer rate increases by convection is dominant in the vicinity of the edges of the obstacle. Keshtkar and Ghazanfari [11] numerically investigated of fluid flow and heat transfer inside an enclosure with three hot obstacles under the influence of magnetic field. They concluded that heat transfer rate in free convection is much higher than in forced convection. Rahman *et al.* [12] studied computational analysis of mixed convection in a channel with a cavity heated from different sides. They observed that highest heat transfer is gained when the isothermal heater is located at the right vertical wall. Fluid flow due to mixed convection in a lid-driven cavity having a heated circular hollow cylinder is numerically analyzed by Billah *et al.* [13]. They found that the flow field and temperature distribute strongly depend on the cylinder diameter and also the solid fluid thermal conductivity ratio at the three convective regions. Sivanandam *et al.* [14] studied hydro-magnetic combined convection in a lid-driven cavity with sinusoidal boundary conditions on both side walls. They found that flow behavior and heat transfer rate inside the cavity are strongly affected by the presence of the magnetic field. MHD mixed convection in a lid-driven cavity with corner heater is analyzed by oztop *et al.* [15]. Basak *et al.* [16] performed the mixed convection flows within a square cavity with linearly heated side walls. Ching *et al.* [17] investigated a finite element simulation of mixed convection heat and mass

transfer in a right triangular enclosure. They found that heat and mass transfer rate increases for all values of Richardson number ( $Ri$ ) and for each direction of the sliding wall motion due to increases of buoyancy ratio. Khanafer and Aithal [18] studied laminar mixed convection flow and heat transfer characteristics in a lid-driven cavity with a circular cylinder. They observed that placing the cylinder near the bottom Nusselt number ( $Nu$ ) where moving the cylinder near the top wall resulted in the lowest average Nusselt number on the bottom wall. Omary [19] reported on the CFD simulations of lid-driven cavity flow at moderate Reynolds number. He concluded that the dynamics and structure of primary vortex are strongly affected by Reynolds number as well as aspect ratio of the cavity.

Biswas *et al.* [20] studied the importance of using adiabatic block inside a lid-driven cavity to enhance thermal energy transport. They showed that the presence of an adiabatic block possibly suppresses the energy circulation. Guo and Sharif [21] investigated mixed convection in rectangular cavities at various aspect ratios with moving isothermal sidewalls and constant heat source. They observed that for asymmetric placement of the heat source, the maximum temperature decreases and the average Nusselt number ( $Nu$ ) increases as the source is moved more and more towards the sidewall. Mousa [22] investigated the laminar buoyancy convection in a square cavity with an obstacle. He found that the rate of heat transfer decreases when the aspect ratio of the adiabatic square obstacle increases. Rahman and Alim [23] investigated MHD mixed convection flow in a vertical lid-driven square enclosure including a heat conducting horizontal circular cylinder with joule heating. They found that mixed convection parameter, the Richardson number ( $Ri$ ) affects significantly on the flow structure and heat transfer inside the enclosure. Also, they found that over all heat transfer rate decreases with increasing joule heater parameter  $J$ . Abraham and Varghese [24] investigated mixed convection in a differentially heated square cavity with moving lids. They found that both inertia and buoyancy forces contribute to the flow structure. Kosti and Rathore [25] studied numerically of lid-driven cavity at different Reynolds number. They investigated that peak of the velocity profiles are increasing with increment in Reynolds number and counter rolling rolls has been found for vertical velocity contours. Zheng *et al.* [26] studied numerically on mixed convection in a lid-driven cavity with a circular cylinder; they

found that the fluid flow and heat transfer characteristics in the cavity strongly depend on the position of circular cylinder. Hussein and Hussain [27] performed mixed convection through a lid-driven air filled square cavity with a hot wavy wall. They showed that the average Nusselt number ( $Nu$ ) remains invariant when the Richardson number ( $Ri$ ) is high. YadollahiFarsani and Ghasemi [28] investigated magnetohydrodynamic mixed convective flow in a cavity. They found that for various Reynolds number, the value of average Nusselt number ( $Nu$ ) decreases as Hartmann number ( $Ha$ ) increases.

## **1.5 Motivation**

From the literature review it is clear that very little numerical study on MHD mixed convection heat transfer in lid-driven enclosure with block have been carried out. The study of MHD mixed convection in lid-driven enclosure with inner block is important for numerous engineering applications. These applications includes cooling of electronic equipments, nuclear reactors, solar collectors, electrical, microelectronic equipments containers and in many other design problems mixed convection heat transfer is pronominent. Thus the analysis of the effect of MHD mixed convection for different boundary conditions and shapes are necessary to ensure efficient performance of heat transfer equipments. On the other hand, the majority of the mixed convection studies were carried out in channel with inner obstacle and natural convection studies were carried out in closed cavities with inner obstacle. Thus far, none have conducted studies involving the effect of MHD mixed convection flow in a lid-driven partially heated rectangular enclosure containing an adiabatic block, although they are widely used. Numerical studies are therefore essential to observe the variation in fluid flow and heat transfer due to the above physical changes, which forms the basis of the motivation behind the present study.

## **1.6 Present Research**

Previously no research has been reported for the actual heat transfer and fluid flow augmentation in lid-driven partially heated enclosure with inner adiabatic block. So the present study is a numerical investigation on the partially heated lid driven enclosure with inner obstacle for the purpose of actual heat transfer and fluid flow

augmentation. In the present investigation, a horizontal lid-driven partially heated rectangular enclosure with inner block is considered. In this enclosure, the top and bottom walls are assumed to be adiabatic while the left and the right walls are maintained at constant temperatures. The top adiabatic wall of the enclosure is allowed to move in its own plane in the direction of positive left to right at a constant velocity. A magnetic field is applied in the horizontal direction parallel to the moving wall in the enclosure. An adiabatic obstacle is displaced inside the enclosure. The proposed studies are expected to reveal that the heat transfers in such arrangements are different from those studied in the above literature and it will therefore prove useful from the designer's point of view in choosing the best physical condition that suits him.

## **1.7 Objectives**

The overall aim of this thesis is to investigate numerically the fluid flow and heat transfer behaviors inside enclosure as stated in previous section. The investigations are to be carried out at different non-dimensional governing parameters such as Reynolds number, Richardson number, Prandtl number, Hartmann number and physical parameters such as elliptical size. The effect of the non-dimensional parameters on overall heat transfer, velocity and temperature distribution will be examined both qualitatively and quantitatively. Results will be presented in terms of streamlines, isotherms, as well as the average Nusselt number, on the heated portion in the enclosure for different values of the governing and the geometric parameters. However, the specific aims of the study are as follows:

- To develop a mathematical model for the effect of magnetohydrodynamic mixed convection flow in a partially heated rectangular lid-driven enclosure with a block and hence to solve that model using finite element method.
- To carry out the validation of the present finite element model by investigating the effect of MHD mixed convection flow within a square enclosure containing a triangular obstacle.
- To investigate the effect of Reynolds number, Richardson number, Prandtl number, as well as the size of the block on the fluid flow and heat transfer characteristics in the enclosure.



- To observe the streamline and isotherms profile as well as overall heat transfer rate from the heat source for above-mentioned parameters.
- To compare the numerical results with different Richardson number for the above mentioned parameters.

### **1.8 Outline of the Thesis**

This dissertation contains five chapters. In this chapter a brief introduction is presented with aim and objective. There is nothing new to say about it. This chapter also consists of a literature review of the past studies on fluid flow and heat transfer in cavities or channels. In this state-of-the art review, different aspects of the previous studies have been mentioned categorically. This is followed by the post-mortem of a recent historical event for the illustration of fluid flow and heat transfer effects in cavities or channels.

Chapter 2 presents the computational details of the problem for viscous incompressible flow.

In Chapter 3, a detailed of mathematical model along with the computational procedure of the problem.

Results as well as discussion are presented in Chapter 4.

Finally, in Chapter 5, the dissertation is rounded off with the conclusions and recommendations for further study of the present problem are outlined.

# Chapter 2

## Computational Details

---

A mathematical model of physical phenomena may be ordinary or partial differential equations, which are used to analyze and numerically investigate. The partial differential equations of fluid mechanics and heat transfer are solvable for only a limited number of flows. To obtain an approximate solution numerically, we have to use a discretization method, which approximates the differential equations by a system of algebraic equations, which can then be solved on a computer. The approximations are applied to small domains in space and /or time so the numerical solution provides results at discrete locations in space and time. Much as the accuracy of experimental data depends on the quality of the tools used, the accuracy of numerical solutions depend on the quality of discretization used.

Computational fluid dynamics (CFD) is a branch of fluid mechanics that uses numerical investigations and data structures to analyze and solve problems involving fluid flows. CFD is applied to a wide range of research and engineering problems in many fields of study and industries including aerodynamics and aerospace analysis, weather simulation, natural science and environmental engineering, industrial system design and analysis, biological engineering and fluid flows, and engine and combustion analysis. Thereby, engineers need CFD codes that can make physically realistic results with good quality accuracy in simulations with finite grids. Contained within the broad field of computational fluid dynamics are activities that cover the range from the automation of well-established engineering design methods to the use of detailed solutions of the Navier-Stokes equations as substitutes for experimental research into the nature of complex flows. It is more frequently used in fields of engineering where the geometry is complicated or some important feature that cannot be dealt with standard methods. More details are available in Ferziger & Perić [36] and Patankar [33].

## 2.1 Advantages of Numerical Investigation

The study of fluid flow and heat transfer in thermodynamics can be performed either theoretically or experimentally. Experimental investigation of such problem could not obtain that much popularity in the field of thermodynamics because of their limited flexibility and applications. For every change of geometry body and boundary condition, it needs separate investigation, involving separate experimental requirement/ arrangement, which, in turn makes it unattractive, especially from the time involved as well as economical point of views. The theoretical investigation on the other hand, can be carried out either by analytical approach or by numerical approach. The analytical methods of solution are not of much help in solving the practical problems. This is mainly due to the very involvement of a large number of variables, complex geometrical bodies, boundary conditions and arbitrary boundary shapes. General closed form solutions can be obtained only for very ideal cases and the results obtained for a particular problem, usually with uniform boundary conditions. For two-dimensional thermodynamics problems, mathematical model involve partial differential equations are required to be solved simultaneously with some boundary conditions. Therefore, there no alternatives accept the numerical methods for the solution of the problems of practical interest. The details are to be had in Fletcher [37] and Patankar [33].

## 2.2 Components of a Numerical Solution Methods

Several components of numerical solution methods are available in Ferziger and Perić [36], here only the main steps will be demonstrated in the following.

### 2.2.1 Mathematical model

For any numerical solution method we have to provide a mathematical model, i.e. the set of partial differential equations and its related boundary conditions. A solution method is usually designed for a particular set of equations. Trying to produce a general-purpose solution method, i.e. one which is applicable to all flows, is impractical, is not impossible and as with most general purpose tools, they are usually not optimum for any one application.

### **2.2.2 Discretization method**

After selecting the mathematical model, one has to choose a suitable discretization method, i.e. a method of approximating the differential equations by a system of algebraic equations for the variable at some set of discrete locations in space and time.

### **2.2.3 Numerical grid**

The next step is to select a numerical grid that defines the discrete locations, at which the variables are to be calculated. It is essentially a discrete representation of the geometric domain on which the problem is to be solved. It divides the solution domain into a finite number of sub-domains such as elements, control volumes etc. Some of the options available are structural (regular) grid, block structured grid, unstructured grids etc.

### **2.2.4 Finite approximations**

After the selection of grid type, one has to choose the approximations to be used in the discretization process. Approximations for the derivatives at the grid points have to be selected in a finite difference method. In a finite volume method, one has to select the methods of approximating surface and volume integrals. In a finite element method, one has to choose the functions and weighting functions.

### **2.2.5 Solution method**

The form of discretization yields a large system of non-linear algebraic equations. The method of solution depends on the type of a problem. For unsteady flows, methods based on those used for initial value problems for ordinary differential equation (marching in time) is used. At each time step an elliptic problem has to be solved. Pseudo-time marching or an equivalent iteration scheme usually solves steady flow problems. Since the equations are non-linear, an iteration scheme is used to solve them. These methods use successive linearization of the equations and the resulting linear systems are almost always solved by iterative techniques. The choice of solver depends on the grid type and the number of nodes involved in each algebraic equation.

## 2.3 Discretization Approaches

To solve a mathematical model of physical phenomena numerically one is to consider numerical discretization. This means that each component of the differential equations is transformed into a “numerical analogue” which can be represented in the computer and then processed by a computer program, built on some algorithm. There are many different methodologies were devised for this purpose in the past and the development still continues. Some special methods are Finite Difference Method (FDM), Finite Volume Method (FVM), Finite Element Method (FEM), Boundary Element Method (BEM) and Boundary Volume Method(BVM).

Galerkin’s finite element method (FEM) has been used in the present numerical computation. Detailed discussion of this method is available in Chung [31] and Dechaumphai [32].

### 2.3.1 Finite element method

The finite element method (FEM) is a powerful computational technique for solving problems, which are described by partial differential equations. This computational technique in which a given domain is represented as a collection of simple domains, called finite elements, for which it is possible to systematically construct the approximation functions needed in the solution of partial differential equations by the weighted residual method. The computational domains with irregular geometries by a collection of finite elements make the method a valuable practical tool for the solution of boundary value problems arising in various fields of engineering. The approximation functions, which satisfy the governing equations and boundary conditions, are often constructed using ideas from interpolation theory. Approximating functions in finite elements are determined in terms of nodal values of a physical field, which is required. A continuous physical problem is transformed into a discretized finite element problem with unknown nodal values. For a linear problem, a system of linear algebraic equations should be solved. Values inside finite elements can be recovered using nodal values.

The finite element method is one of the numerical methods that have received popularity due to its capability for solving complex structural problems. The method has been extended to solve problems in several other fields such as in the field of

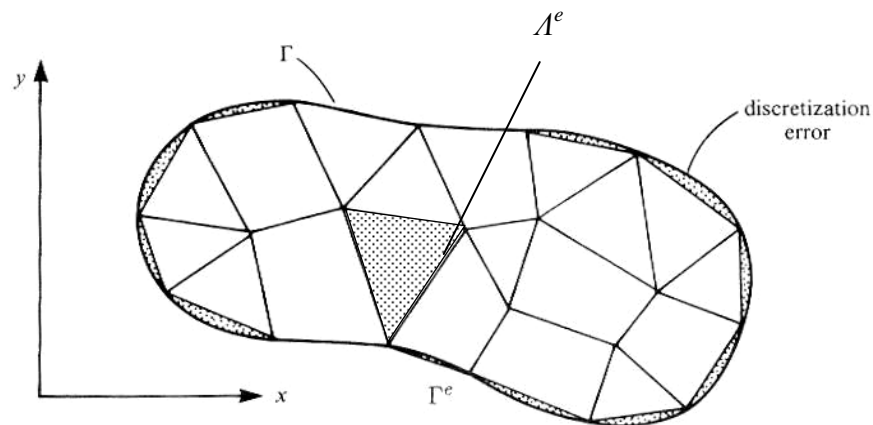
heat transfer, computational fluid dynamics, electromagnetic, biomechanics etc. In spite of the great success of the method in these fields, its application to fluid mechanics, particularly to convective viscous flows, is still under intensive research.

The major steps involved in finite element analysis of a typical problem are:

1. Discretization of the given domain into a set of finite elements (mesh generation).
2. Weighted-integral or weak formulation of the differential equation to be analyzed.
3. Development of the finite element model of the problem using its weighted-integral or weak form.
4. Assembly of finite elements to obtain the global system of algebraic equations.
5. Imposition of boundary conditions.
6. Solution of equations.
7. Post-computation of solution and quantities of interest.

### 2.3.2 Grid generation

The arrangement of discrete points throughout the flow field is simply called a grid. The determination of a proper grid for the flow through a given geometric shape is important. The way that such a grid is determined is called grid generation. The grid generation is a significant consideration in CFD. Finite element method can be applied to unstructured grids. This is because the governing equations in this method are written in integral form and numerical integration can be carried out directly on the unstructured grid domain in which no coordinate transformation is required. A two-dimensional domain may be triangulated as shown in Figure 2.1. In finite element method, the mesh generation is the technique to subdivide a domain into a set of sub-domains, called finite elements. Figure 2.1 shows a domain,  $A$  is subdivided into a set of sub-domains,  $A^e$  with boundary  $\Gamma^e$ . Detailed discussion of this issue is available in Anderson [29] and Chung [31].



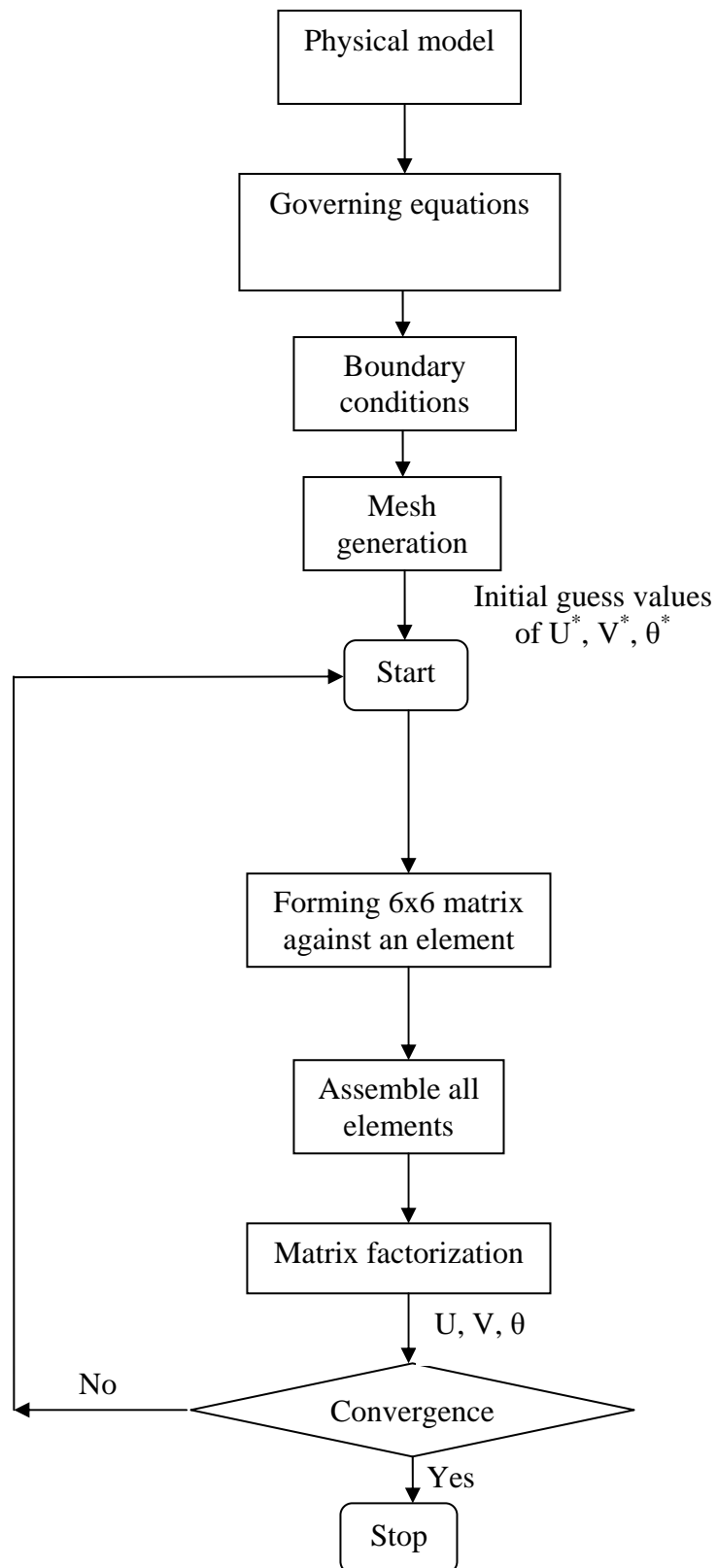
**Figure 2.1:** A typical FE discretization of a domain, Reddy & Gartling [38].

### 2.3.3 Finite element formulation and computational procedure

Viscous incompressible thermal flows have been the subject of our investigation. The problem is relatively complex due to the coupling between the energy equation and the Navier-Stokes equations, which govern the fluid motion. These equations comprise a set of coupled nonlinear partial differential equations, which is difficult to solve especially with complicated geometries and boundary conditions. The finite element formulation and computational procedure for Navier-Stokes equations along with energy equations will be discussed in the chapter 3.

### 2.3.4 Algorithm

The algorithm was originally put forward by the iterative Newton-Raphson algorithm; the discrete forms of the continuity, momentum and energy equations are solved to find out the value of the velocity and the temperature. It is essential to guess the initial values of the variables. Then the numerical solutions of the variables are obtained while the convergent criterion is fulfilled. The simple algorithm is shown by the flow chart below.



**Figure 2.2:** Flow chart of the computational procedure



# Chapter 3

## Mathematical Modeling

---

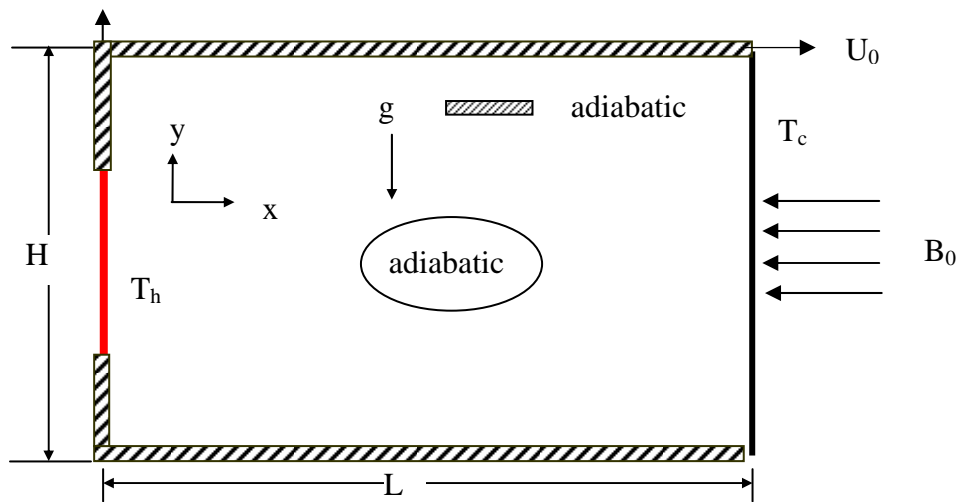
### 3.1 General

Mixed convective heat transfer within rectangular enclosure is a function of the difference between the hot and cold walls, the boundary conditions, the position of heater on the enclosure and the properties of conducting fluid flow.

The generalized governing equations are used based on the conservation laws of mass, momentum and energy. As the heat transfer depends upon a number of factors, a dimensional analysis is presented to show the important non-dimensional parameters which will influence the dimensionless heat transfer parameter, i.e. average Nusselt number.

### 3.2 Physical Configuration

The physical model of the system and coordinates have been shown in figure 3.1. A Cartesian co-ordinate system has been used with origin at the lower left corner of the computational domain. It is a two dimensional rectangular lid-driven enclosure with an adiabatic elliptic block filled with electrically conducting fluid. The top adiabatic wall of the enclosure has been allowed to move from left to right in its own plane at a constant velocity,  $U_0$ . The partially left wall of the enclosure has been supposed at high temperature,  $T_h$ , whereas the right wall has been maintained at low temperature,  $T_c$  while the remaining walls have been kept adiabatic. The gravitational force acts in the vertically downward direction and a uniform magnetic field of strength,  $B_0$  has been applied along the horizontal direction.



**Figure 3.1:** The schematic diagrams of partially heated lid-driven rectangular enclosure with an elliptical block.

### 3.3 Mathematical Formulation

The several steps of the mathematical formulation for the above physical configurations are shown as follows

#### 3.3.1 Governing equations

The generalized governing equations are used to solve the fluid flow and heat transfer problems are the conservation of mass (continuity equations), conservation of momentums (momentum equations), and conservation of energy (energy equations), which constitute a set of coupled, nonlinear, partial differential equations. For laminar incompressible thermal flow, the buoyancy force is included here as a body force in the  $v$ -momentum equation. The governing equations for the two-dimensional steady flow after invoking the Boussinesq approximation and neglecting radiation and viscous dissipation can be expressed as

Continuity Equation

$$\frac{\partial u}{\partial x} + \frac{\partial v}{\partial y} = 0 \quad (3.1)$$

Momentum Equations

$$u \frac{\partial u}{\partial x} + v \frac{\partial u}{\partial y} = -\frac{1}{\rho} \frac{\partial p}{\partial x} + \nu \left( \frac{\partial^2 u}{\partial x^2} + \frac{\partial^2 u}{\partial y^2} \right) \quad (3.2)$$

$$u \frac{\partial v}{\partial x} + v \frac{\partial v}{\partial y} = -\frac{1}{\rho} \frac{\partial p}{\partial y} + \nu \left( \frac{\partial^2 v}{\partial x^2} + \frac{\partial^2 v}{\partial y^2} \right) + g\beta(T - T_c) - \frac{\sigma B_0^2 v}{\rho} \quad (3.3)$$

Energy Equations

$$u \frac{\partial T}{\partial x} + v \frac{\partial T}{\partial y} = \frac{k}{\rho c_p} \left( \frac{\partial^2 T}{\partial x^2} + \frac{\partial^2 T}{\partial y^2} \right) \quad (3.4)$$

where  $x$  and  $y$  are the distances measured along the horizontal and vertical directions respectively;  $u$  and  $v$  are the velocity components in the  $x$  and  $y$  directions respectively;  $T$  denotes the fluid temperature,  $T_c$  denotes the reference temperature for which buoyant force vanishes,  $p$  is the pressure and  $\rho$  is the fluid density,  $g$  is the gravitational constant,  $\beta$  is the volumetric coefficient of thermal expansion,  $c_p$  is the fluid specific heat.

### 3.3.2 Boundary conditions

The boundary conditions for the present problem can be written as follows:

At the left wall:  $u = 0, v = 0, T = T_h$

At the right vertical wall:  $u = 0, v = 0, T = T_c$

At the elliptical and bottom walls:  $u = 0, v = 0, \frac{\partial T}{\partial y} = 0$

At the top wall:  $u = U_0, v = 0, \frac{\partial T}{\partial y} = 0$

Heat transfer rate is measure by local and average value of Nusselt number. Local Nusselt number at the heated surface of the enclosure defined by Cengel [30] is calculated by using the equations:

$$Nu_l = h(y)L/k$$

The average value of Nusselt number is calculated by integrating the local value over the total length of the hot wall using the relation.

$$Nu = \frac{1}{L_s} \int_0^{L_s} Nu_l dy$$

Where  $L_s$  and  $h(y)$  are the length and the local convection heat transfer coefficient of the heated wall respectively

### 3.3.3 Dimensional analysis

Non-dimensional variables are used for making the governing equations (3.1–3.4) into dimensionless form are stated as follows:

$$X = \frac{x}{L}, Y = \frac{y}{L}, U = \frac{u}{U_0}, V = \frac{v}{V_0}, P = \frac{p}{\rho U_0^2}, \theta = \frac{(T - T_c)}{(T_h - T_c)},$$

where  $X$  and  $Y$  are the coordinates varying along horizontal and vertical directions, respectively,  $U$  and  $V$  are the velocity components in the  $X$  and  $Y$  directions, respectively,  $\theta$  is the dimensionless temperature and  $P$  is the dimensionless pressure. After substitution the dimensionless variables into the equations (3.1-3.4), we get the following dimensionless equations as

Continuity Equation

$$\frac{\partial U}{\partial X} + \frac{\partial V}{\partial Y} = 0 \quad (3.5)$$

Momentum Equations

$$U \frac{\partial U}{\partial X} + V \frac{\partial U}{\partial Y} = -\frac{\partial P}{\partial X} + \frac{1}{Re} \left( \frac{\partial^2 U}{\partial X^2} + \frac{\partial^2 U}{\partial Y^2} \right) \quad (3.6)$$

$$U \frac{\partial V}{\partial X} + V \frac{\partial V}{\partial Y} = -\frac{\partial P}{\partial Y} + \frac{1}{Re} \left( \frac{\partial^2 V}{\partial X^2} + \frac{\partial^2 V}{\partial Y^2} \right) + Ri \theta - \frac{Ha^2}{Re} V \quad (3.7)$$

Energy Equations

$$U \frac{\partial \theta}{\partial X} + V \frac{\partial \theta}{\partial Y} = \frac{1}{Re Pr} \left( \frac{\partial^2 \theta}{\partial X^2} + \frac{\partial^2 \theta}{\partial Y^2} \right) \quad (3.8)$$

The dimensionless parameters appearing in the equations (3.5) through (3.8) are the Reynolds number ( $Re$ ), Grashof number ( $Gr$ ), Prandtl number ( $Pr$ ), and Richardson number ( $Ri$ ). They are respectively defined as follows:

$$Re = UL/\nu, Gr = g \beta \Delta T L^3 / \nu^2, Pr = \nu/\alpha, \text{ and } Ri = Gr/Re^2$$

where  $\Delta T = T_h - T_c$  and  $\alpha = k/\rho C_p$  are the temperature difference and thermal diffusivity of the fluid respectively.

The dimensionless boundary conditions under consideration can be written as:

$$\text{At the heated left vertical wall: } U = 0, V = 0, \theta = 1$$

$$\text{At the right vertical wall: } U = 0, V = 0, \theta = 0$$

$$\text{At the top walls: } U = 1, V = 0, \frac{\partial \theta}{\partial Y} = 0$$

$$\text{At the elliptical and bottom walls: } U = 0, V = 0, \frac{\partial \theta}{\partial Y} = 0$$

where  $K$  is the thermal conductivity. The average Nusselt number at the heated wall of the enclosure based on the no-dimensional variables may be expressed

$$\text{as } Nu = -\frac{1}{L_h} \int_0^{L_h/L} \frac{\partial \theta}{\partial X} dY. \text{ Where } L_h \text{ is length of the heated portion of the enclosure.}$$

### 3.3.4 Grid sensitivity test

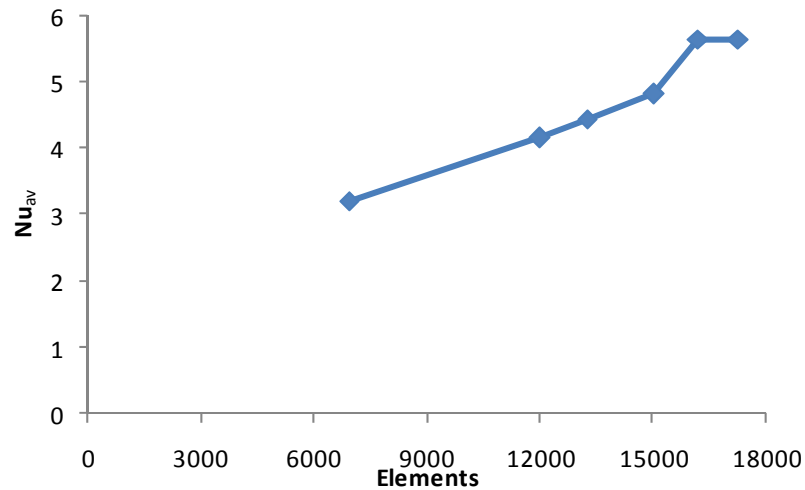
The grid sensitivity tests are examined to find the variables grid independence solution. Triangular element grid system is employed in the present study. Several grid size sensitivity tests are carried in this geometry to determine the sufficiency of the mesh scheme and to ensure that the solutions are grid independent. This is obtained when numerical results of the average Nusselt number ( $Nu$ ) of the fluid and solution time become grid size independent, although we continue the refinement of the mesh grid. Six different non-uniform grids with the following number of nodes and elements were considered for the grid refinement tests: 3484 nodes, 6929 elements; 6049 nodes, 12024 elements; 6684 nodes, 13281 elements; 7584 nodes, 15052 elements, 8313 nodes, 16232 elements and 8717 nodes, 17300 elements as shown in Table 3.1. Considering both the accuracy and the computational time, the

values, 8313 nodes and 16232 elements can be chosen throughout the simulation to optimize the relation between the accuracy required and the computing time.

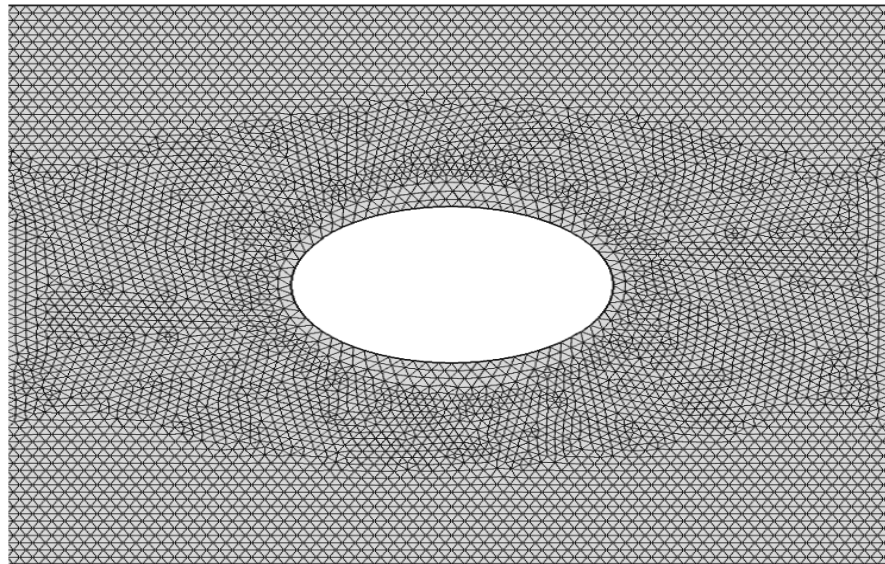
In finite element method, the mesh generation is the technique to subdivide a domain into a set of sub-domains, called finite elements, control volume etc. The numerical grid defines the discrete locations, at which the variables are to be calculated, which is essentially a discrete representation of the geometry domain on which the problem is to be solved. Unstructured triangular grids are used in the present finite element simulation. The mesh mode for this problem generated by the Delaunay Triangular Method. The Delaunay triangulation is a geometric structure that has enjoyed great popularity in mesh generation since the mesh generation was in its infancy. In two dimensions, the Delaunay triangulation of a vertex set maximizes the minimum angle among all possible triangulations of that vertex set. The mesh modes for the present numerical computation are shown in The mesh mode for the present numerical computation is shown in figure 3.3.

**Table 3.1:** Grid sensitivity check at  $Re = 100$ ,  $Ri = 1.0$ ,  $Ha = 10$  and  $Pr = 0.71$

Nodes	3484	6049	6684	7584	8313	8717
(elements)	(6929)	(12024)	(13281)	(15052)	(16232)	(17300)
$Nu_{av}$	3.2079	4.1578	4.4367	4.8170	5.6469	5.6472
Time (s)	3	4	4	5	5	7



**Figure 3.2:** Grid sensitivity test at  $Ri = 1$ ,  $Re = 100$ ,  $Ha = 10$  and  $Pr = 0.71$

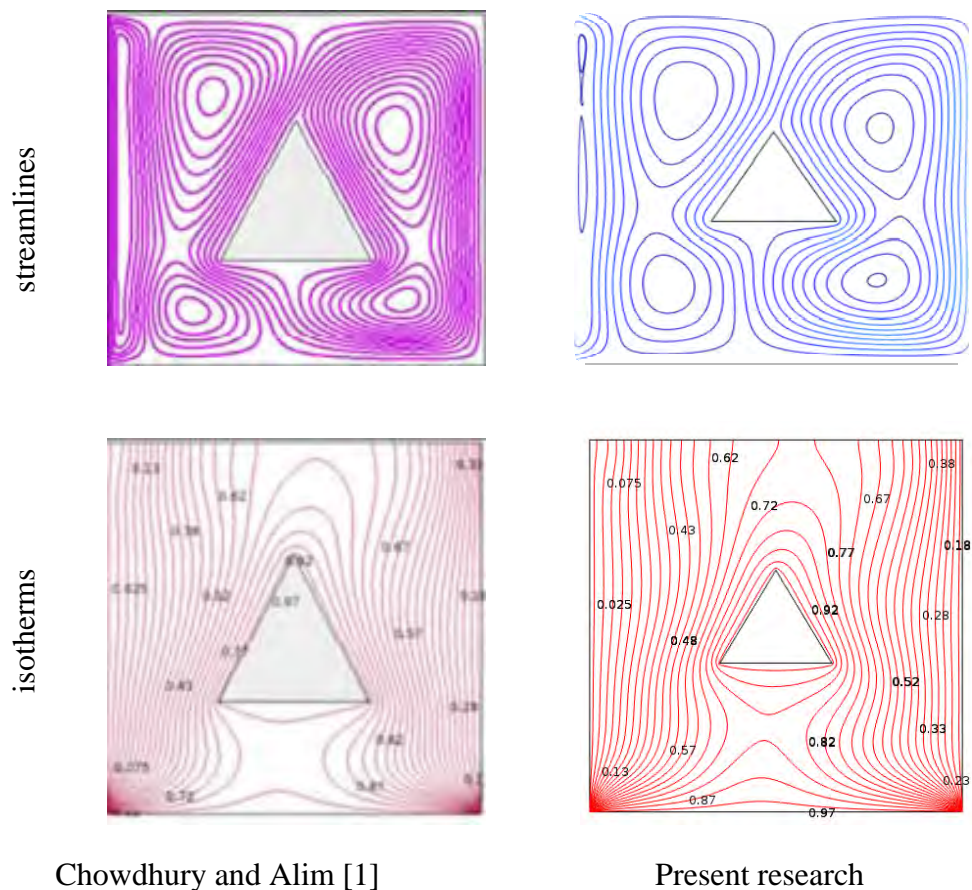


**Figure 3.3:** Mesh structure with 8313 numbers of nodes for present study.

### 3.3.5 Validation of the numerical scheme

In order to verify the accuracy of the numerical results and the validity of the numerical scheme obtained throughout the present study, comparisons with the previously published results are necessary. But due to the lack of availability of experimental data on the particular problems along with its associated boundary conditions investigated in this study, validation of the predictions could not be done against experiment. The present numerical scheme is validated for analysis of MHD mixed convection flow within a square enclosure containing a triangular obstacle

reported by Chowdhury and Alim [1]. The comparison of the results obtained from present code with of Chowdhury and Alim is demonstrated for  $Ri = 10$ ,  $Ha = 40$ ,  $Re = 100$  and  $Pr = 0.71$ . The physical problem studied in [1] was a square enclosure with length of sides is  $L$ . The vertical left and right walls were cold and bottom wall was heated where top wall was adiabatic. The left wall of the enclosure was allowed to move upward direction in its own plane at a constant velocity  $V_0$ . A heated triangular obstacle was kept at the center of the enclosure. The present result has a good agreement with the result obtained by Chowdhury and Alim [1]. Based on the above study, it is concluded that the numerical scheme could be reliability applied to the considered problem. The stream line and isotherms depicted in figure are similar. It is seen from figure 3.4 that the agreement between the present and previous results is very good.



**Figure 3.4:** Code validation for present research.



# Chapter 4

## Results and Discussions

---

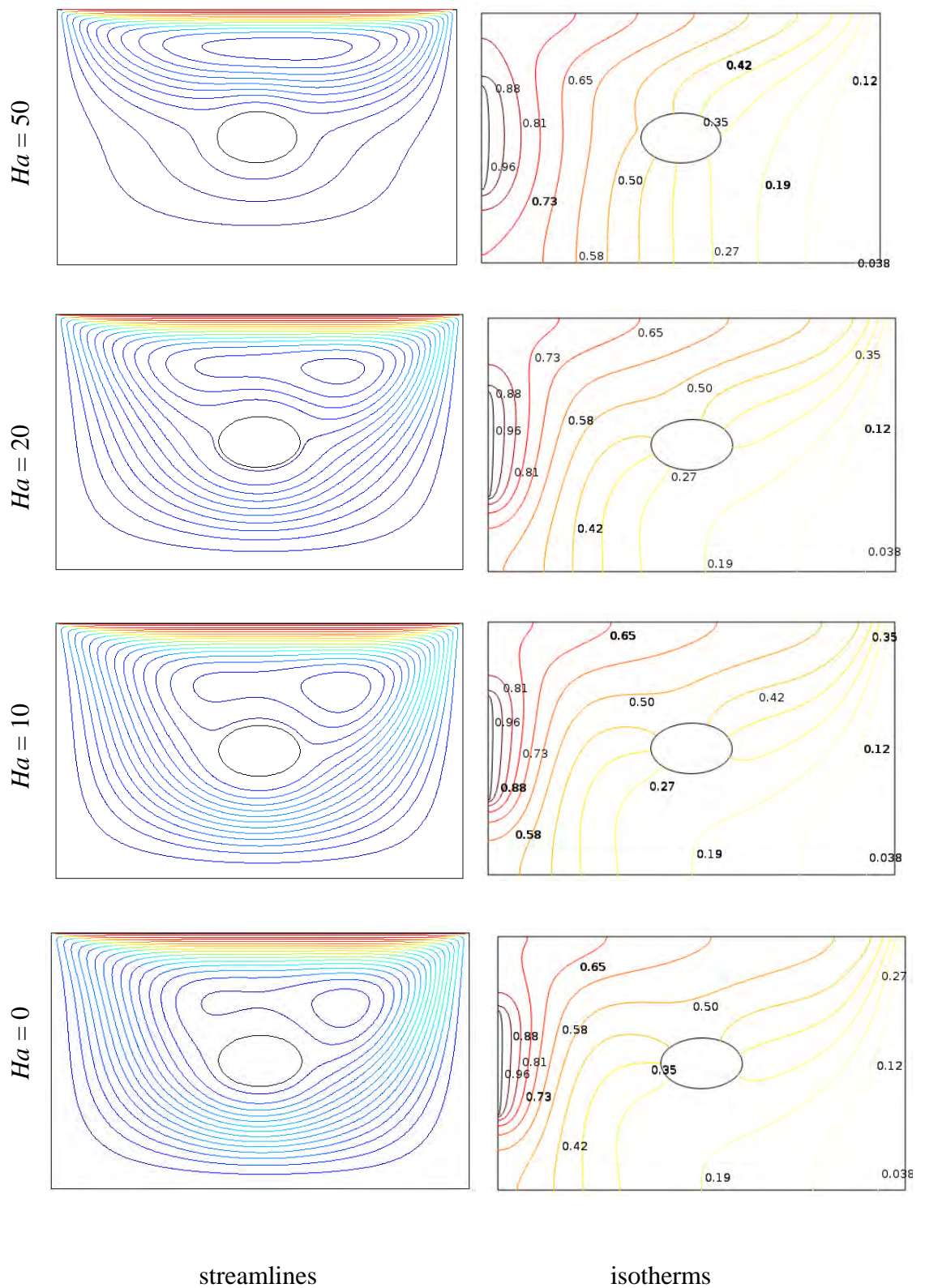
Analysis of MHD mixed convective flow in a lid-driven enclosure has numerous applications in engineering sectors such as materials processing, flow and heat transfer in solar ponds, dynamics of lakes, reservoirs and cooling ponds, crystal growing, float glass production, metal casting, food processing, galvanizing, and metal coating etc. Combined forced and free convective flow in lid-driven cavities occurs as a result of two competing mechanisms. The first is due to shear flow caused by the movement of one of the walls in the enclosure, while the second is due to buoyancy flow produced by thermal non-homogeneity of the enclosure boundaries. When a temperature gradient is imposed such that the shear driven and buoyancy effects are of comparable magnitude then the resulting flow falls under the mixed convection regime and the interaction or coupling of these effects makes the analysis more complex. This problem has been studied in detail in the past. However, the mechanism of heat transfer under such flow in a lid-driven enclosure with the insertion of an elliptical block has not been investigated yet.

In the present chapter the major objective is to perform the effect of magnetohydrodynamic mixed convection flow in a partially heated rectangular lid-driven enclosure with adiabatic elliptic block. The variation of streamlines, isotherms, average Nusselt number at the heated surface for the various relevant dimensionless parameters Hartmann number ( $Ha$ ), Reynolds number ( $Re$ ), Richardson number ( $Ri$ ), Prandtl number ( $Pr$ ), and physical parameter i.e. the area of the elliptical block of the enclosure are shown graphically. In addition, numerical values of the average Nusselt number at the heated surface for the above mentioned parameters have been presented in tabular form.

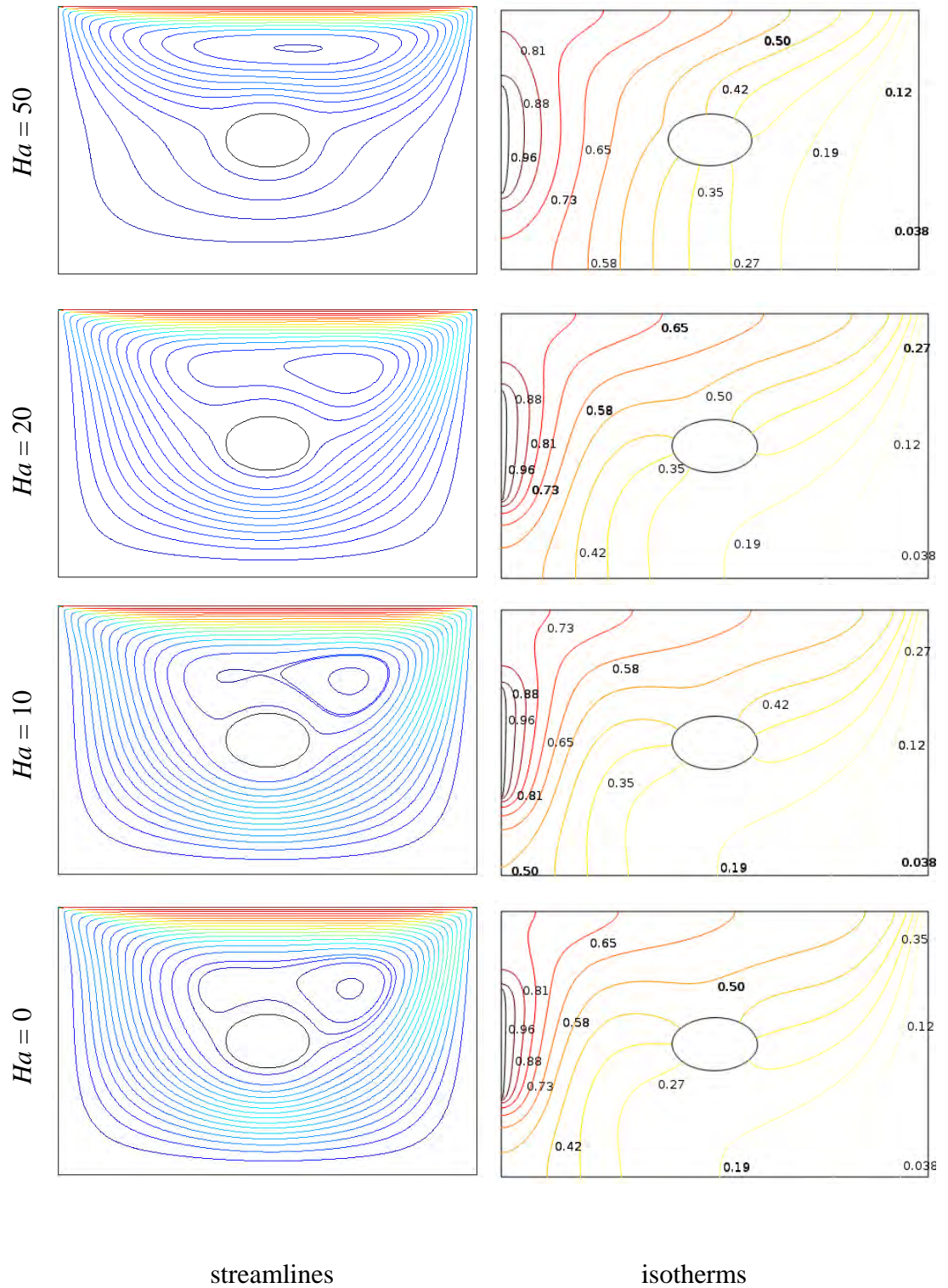
### 4.1 Effect of Hartmann number

The influence of Hartmann number ( $Ha$ ) on the streamlines and isotherms at  $Ri = 0.1, 1.0,$  and  $10$  are shown in the figure 4.1, 4.2, and 4.3 respectively where  $Re = 100$  and  $Pr = 0.71$  are kept fixed. In the absence of the magnetic field ( $Ha = 0$ ) and the forced convection effect ( $Ri = 0.1$ ), from figure 4.1 it is seen that the fluid flow is characterized by a primary rotating unicellular vortex of the size of the enclosure generated by the movement of the top wall. The flow field rise up at the top wall and flow down to the bottom wall of the enclosure due to lidding velocity of the top wall. It is also observed that the vortex of the size remains unchanged of the enclosure with increasing  $Ha$  up to 20. But at  $Ha = 50$ , the vortex of the size is changed and core of the vortex shifted to the oval shape. Also it is found that the flow field is reduced at  $Ha = 50$ , this is expected since presence of magnetic field usually retards the velocity field. From these figures it is clear that the strength of flow is reduced due to increasing Hartmann number. The corresponding effects of Hartmann number ( $Ha$ ) on the isotherms is depicted in the second column of figure.4.1. The temperature field shows that the thermal lines almost parallel to vertical walls for the highest value of  $Ha$  ( $Ha = 50$ ), indicating that most of the heat transfer carried out by conduction. However, some deviations in the conduction dominated isothermal lines are initiated near the right top surface of the enclosure for the value of  $Ha = 10$ . In figure 4.2, when natural convection and forced convection become equally dominant namely  $Ri = 1$ , i.e., in mixed convection, the characteristics of the flow field are almost similar to the characteristics as  $Ri = 0.1$  which is shown in figure 4.1. From isotherms it can be seen that for different values of Hartmann number up to  $Ha = 20$ , there is no remarkable changes. This reveals the fact that still mixed convection dominates the heat transfer mechanism and weak magnetic field does not impact on the heat distribution remarkably. On the other hand, if the Hartmann number is increased to 50, the isotherms seem to be straightened out, i.e., the energy transportation is changed to conduction mode.

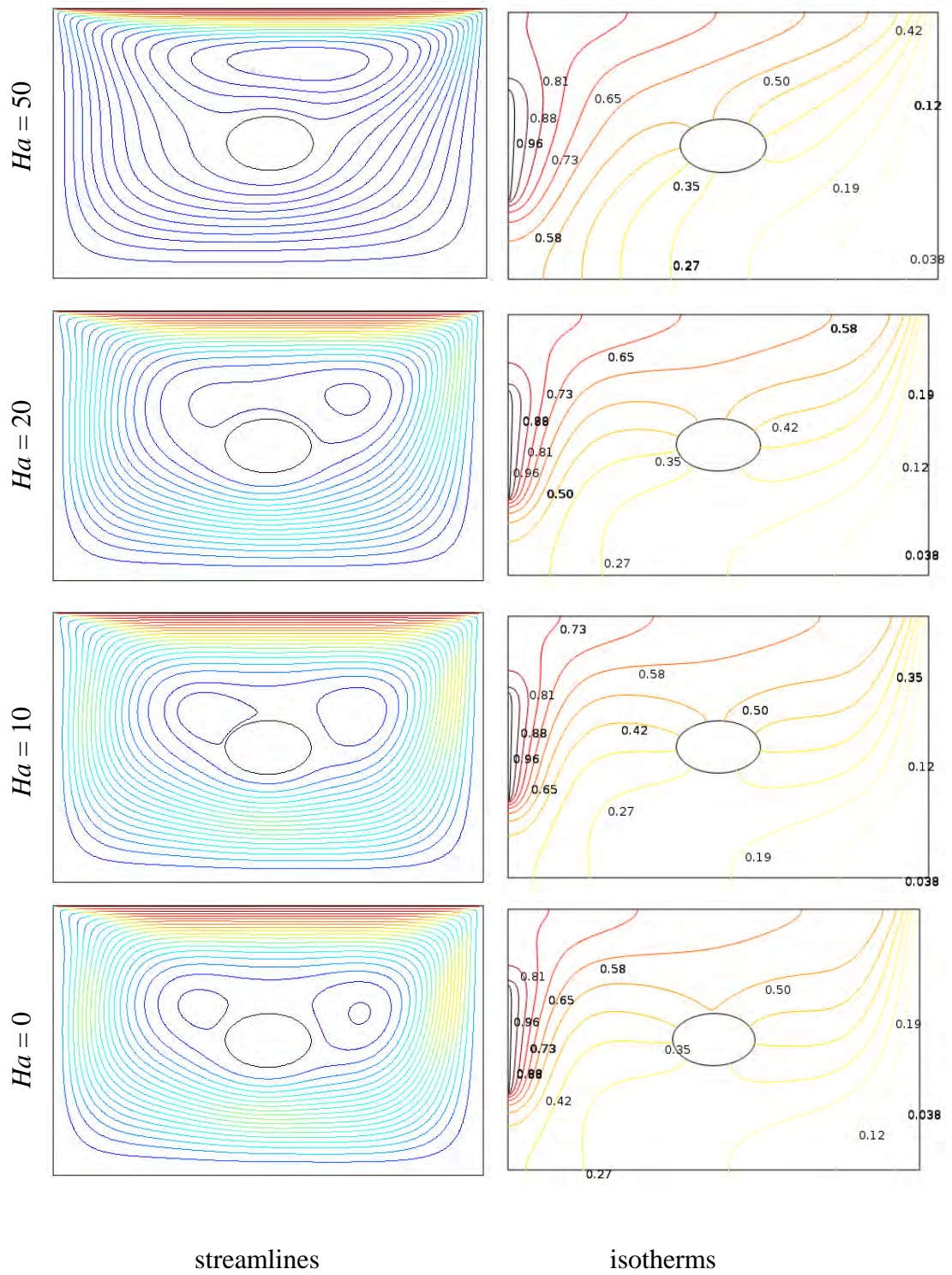
From figure 4.3, it is seen that, when  $Ri = 10$ , i.e. the effect of forced convection is very much less compared to natural convection effect, the velocity field forms two



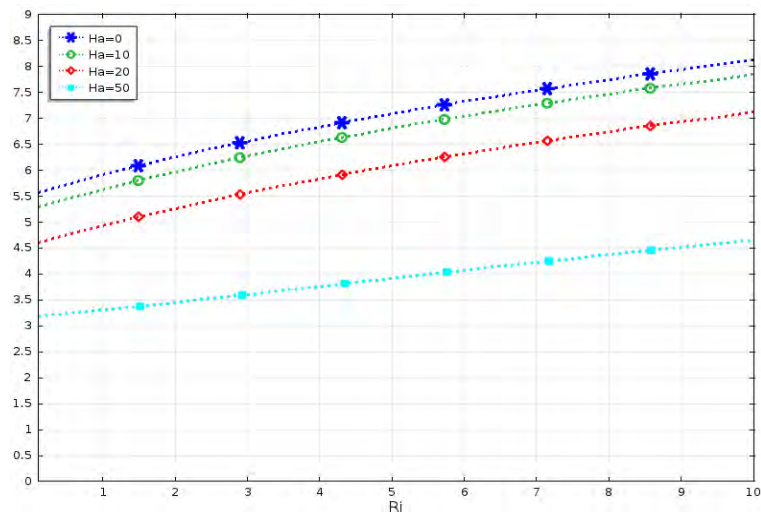
**Figure 4.1:** Effect of Hartmann number on streamlines and isotherms while  $Ri = 0.1$ ,  $Re = 100$ ,  $Pr = 0.71$ .



**Figure 4.2:** Effect of Hartmann number on streamlines and isotherms while  $Ri = 1$ ,  $Re = 100$ ,  $Pr = 0.71$ .



**Figure 4.3:** Effect of Hartmann number on streamlines and isotherms while  $Ri = 10, Re = 100, Pr = 0.71$ .



**Figure 4.4:** Effect of Hartmann Number ( $Ha$ ) on average Nusselt number, while  $Re = 100$ ,  $Pr = 0.71$ .

**Table 4.1:** Variation of the average Nusselt number with Hartmann number for different Richardson number.

$Ri$	$Nu_{av}$			
	$Ha = 0$	$Ha = 10$	$Ha = 20$	$Ha = 50$
0.1	5.57	5.28	4.60	3.18
1	5.91	5.63	4.93	3.30
2	6.25	5.97	5.26	3.45
3	6.56	6.27	5.56	3.60
4	6.83	6.55	5.83	3.76
5	7.09	6.80	6.08	3.92
6	7.32	7.04	6.31	4.07
7	7.54	7.26	6.53	4.22
8	7.74	7.46	6.74	4.37
9	7.94	7.66	6.93	4.51
10	8.12	7.84	7.12	4.65

minor core of the vortex at  $Ha = 0$ . Two minor core of the vortex is formed due to buoyancy force. Size of the two minor core of the vortex increases at  $Ha = 10$ . However, the two minor core of the vertex merge into one and the core shifted oval shape at  $Ha = 50$ . It is seen also that the speed of the fluid is reduced at the higher value of Hartmann number. This is because of the application of transverse magnetic field which tends to slow down the movement of the buoyancy-induced flow in the enclosure. The temperature field depicted the in right column of the figure 4.3. From figures it is seen that the temperature field is drastically changed with decreasing  $Ha$ . At  $Ha = 50$ , the thermal lines of the isotherms are almost parallel to vertical line of the enclosure. The curvedness of the thermal line is increasing with decreasing Hartmann number. In addition, the formation of thermal boundary layers near the cold vertical wall is to be initiated for the lower value of  $Ha$  this is owing to the dominating influence in the enclosure.

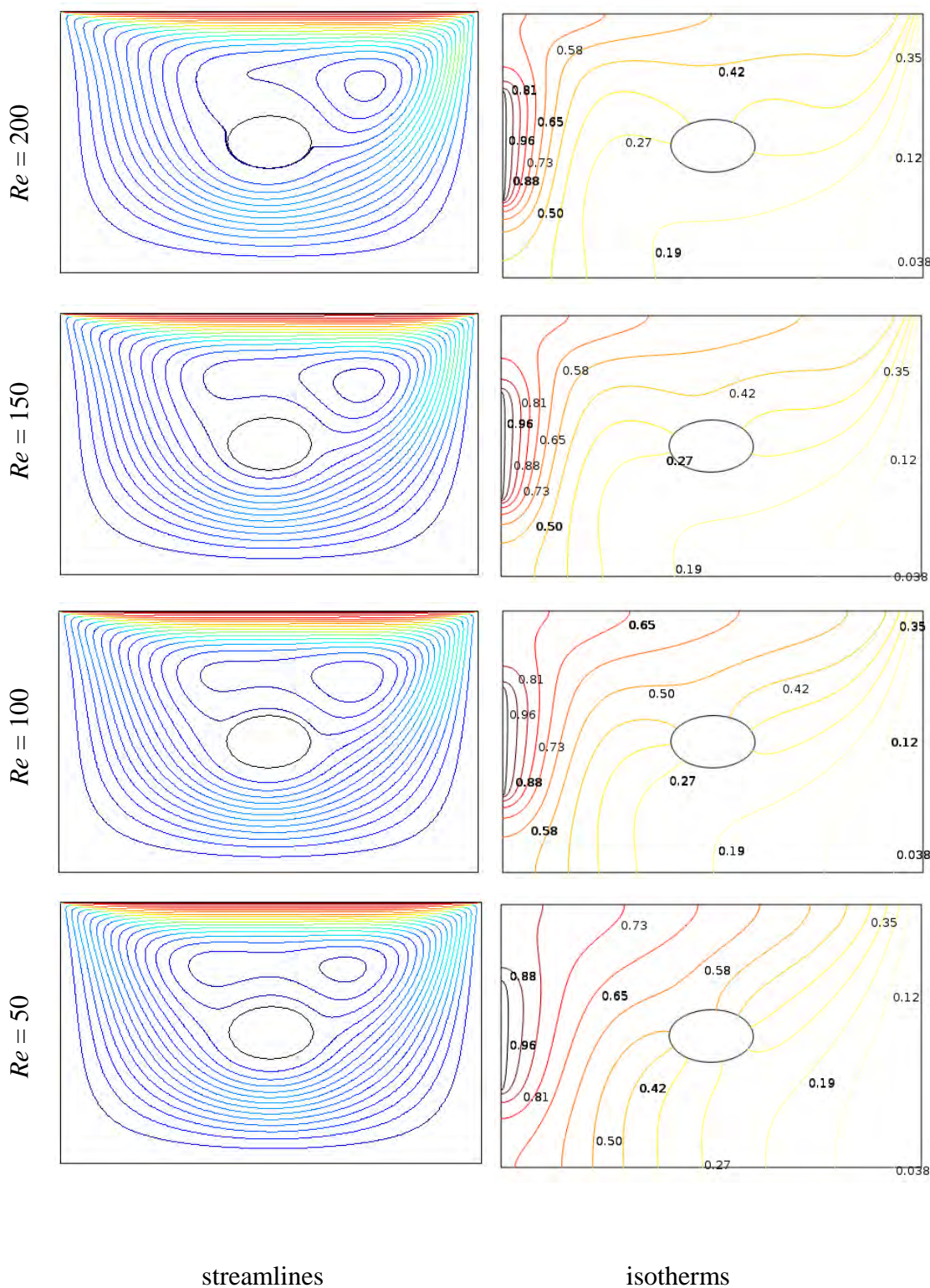
In order to analyze how the presence of magnetic effects heat transfer rate along the hot wall, average Nusselt number ( $Nu$ ) is plotted as a function of Richardson number  $Ri$  and Hartmann number ( $Ha$ ) as shown in figure 4.4.

It is observed that the average Nusselt number ( $Nu$ ) increases as the Richardson number increases and decreases as the Hartmann number increases. From this figure it is noticed that they increase quickly in the mixed to natural convection dominated region for all values of  $Ha$ . But from forced to mixed convection dominated region it increases slowly. This is because the shear driven force weak, so the convection heat transfer is very slight and the conduction is dominated. It is also seen that the average Nusselt number monotonically decreasing with increasing Hartmann number ( $Ha$ ) up to 20. But at Hartmann number  $Ha = 50$ , the average Nusselt number noticeably decreases. Since, the magnetic force is the dominant force and controls the flow inside the enclosure which leads to drop the Nusselt number. Also, in the absence of Hartmann number ( $Ha = 0$ ) the average  $Nu$  is highest. Last of all, the quantitative values of  $Nu$  at different values of  $Ha$  are listed in the Table 4.1. In mixed convection dominated region, the heat transfer decreases 4.74, 16.58, and 44.16% with increasing Hartmann number from  $Ha = 0$  to 10, 20, and 50 respectively. Also in forced convection dominated region, the heat transfer decreases 5.21, 17.41, and 42.91% from  $Ha = 0$  to 10, 20, and 50 respectively.

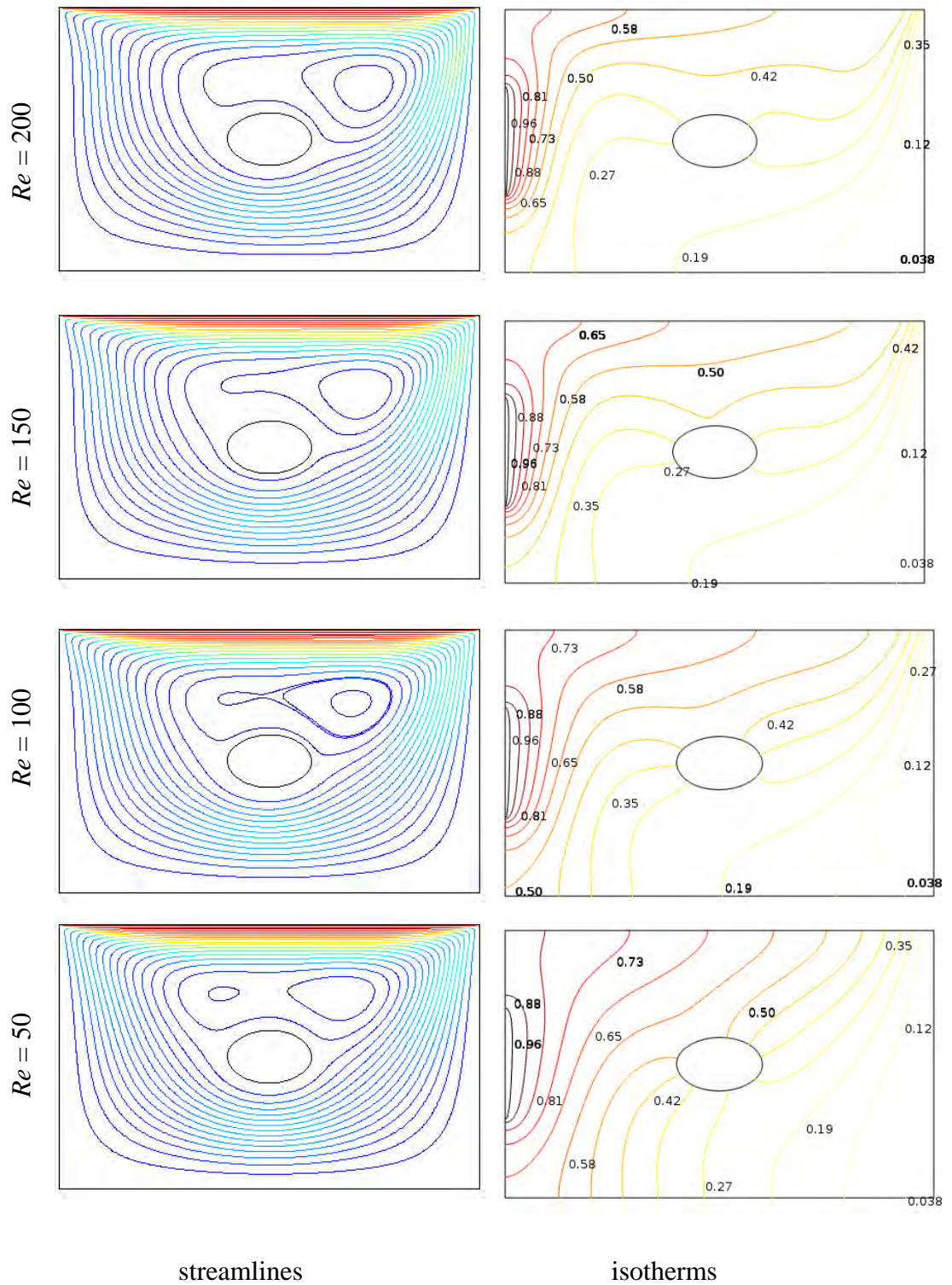
## 4.2 Effect of Reynolds number

The fluid velocity and temperature distribution inside the enclosure are presented in terms of streamlines and isotherms in the figure 4.5, 4.6, and 4.7 at  $Ri = 0.1$ ,  $Ri = 1.0$ , and  $Ri = 10$  respectively with four values of Reynolds number ( $Re = 50, 100, 150$  and  $200$ ) while  $Ha = 10$ ,  $Pr = 0.71$ . At  $Ri = 0.1$ , when forced convection is dominated, the motion of the top wall fluid rise up along the side of adiabatic top wall and flow down along the bottom wall forming a roll with clockwise rotation inside the enclosure which is shown in figure 4.5. At  $Re = 50$ , the rotating cell forms a core of the recirculation cell inside the enclosure and remains unchanged up to  $Re = 100$ . It is observed that the number of core of the recirculation cell increases with increasing Reynolds number. Also, the size of the core of the recirculation cell is increased and crowded towards the right top corner of the enclosure at  $Re = 200$ . The physical meanings behind this fact that the flow of the fluid is increases with increasing Reynolds number. Now we draw the attention to see the effect of increasing Reynolds number ( $Re$ ) on the temperature distribution in the enclosure. From right column of figure 4.5, it can be observed that isothermal lines are nearly parallel to the hot wall at  $Re = 50$ . It remains unchanged up to  $Re = 100$ . At  $Re = 200$ , it is seen that isothermal lines are condensed next to the side walls and isothermal lines are almost parallel to the horizontal line. It is also seen that number of thermal lines is thinner in middle of the enclosure and a thin thermal boundary layer appears at the bottom wall of the enclosure which means increasing heat transfer through convection. In figure 4.6, when both the buoyant force and shear driven force are present in the enclosure namely at  $Ri = 1.0$ , from streamline it can be seen that, at  $Re = 50$ , two minor eddies of primary circulation cells are formed. With increasing Reynolds number two minor eddies merged into one and shifted towards the right top corner of the enclosure. This is occurred because the both buoyancy force and shear force increase the velocity of the motion with increasing Reynolds number. At  $Ri = 1.0$ , from streamline it can be seen that the isotherm patterns reflects a conductive pattern of  $Re$  ( $Re = 50, 100$ ) and a convective pattern of energy transfer at the higher values of  $Re$  ( $Re = 150, 200$ ) for both buoyant force and shear force.

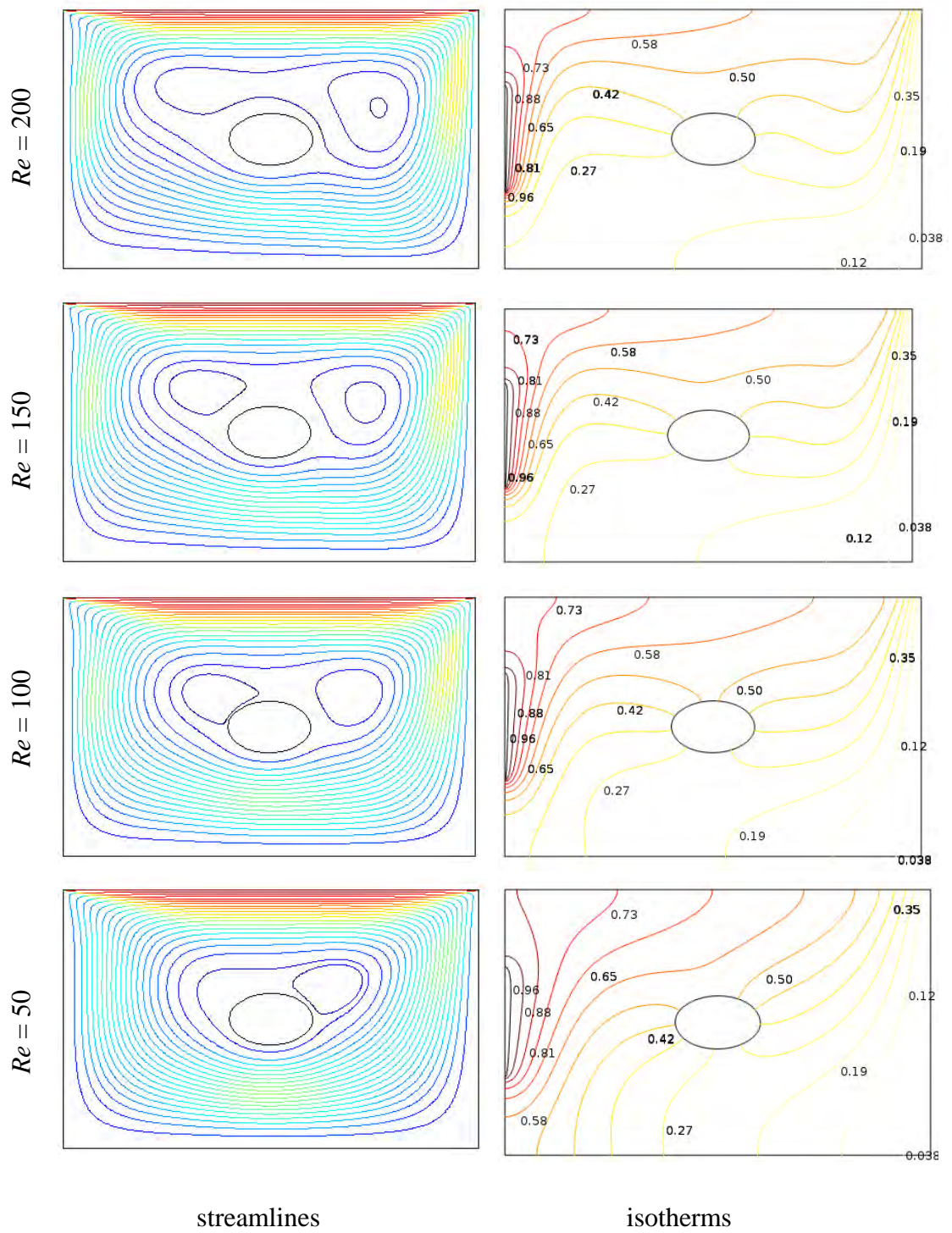




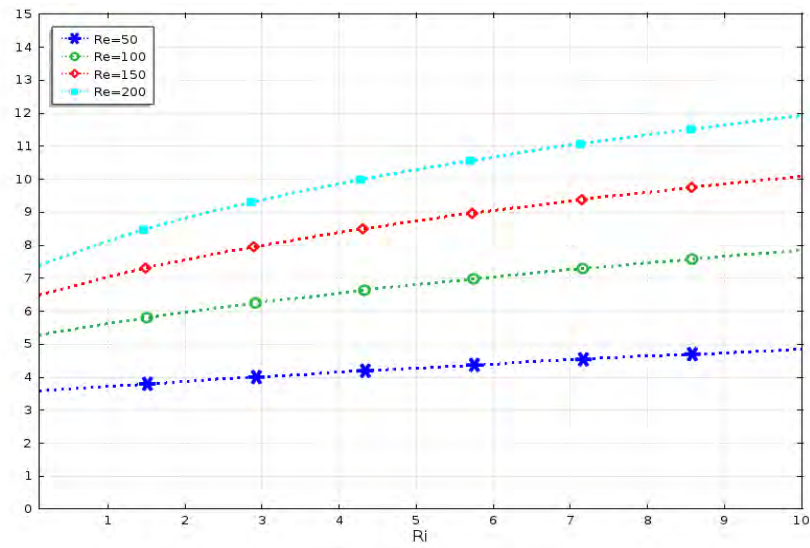
**Figure 4.5:** Effect of Reynolds number on streamlines and isotherms while  $Ri = 0.1$ ,  $Ha = 10$ ,  $Pr = 0.71$ .



**Figure 4.6:** Effect of Reynolds number on streamlines and isotherms while  $Ri = 1$ ,  $Ha = 10$ ,  $Pr = 0.71$ .



**Figure 4.7:** Effect of Reynolds number on streamlines and isotherms while  $Ri = 10$ ,  $Ha = 10$ ,  $Pr = 0.71$ .



**Figure 4.8:** Effect of Reynolds Number  $Re$  on average Nusselt number, while  $Ha = 10$ ,  $Pr = 0.71$

**Table 4.2:** Variation of average Nusselt number with Reynolds number for different Richardson number

$Ri$	$Nu_{av}$			
	$Re = 50$	$Re = 100$	$Re = 150$	$Re = 200$
0.1	3.58	5.28	6.49	7.37
1	3.72	5.63	7.05	8.14
2	3.87	5.97	7.56	8.82
3	4.01	6.28	8.00	9.38
4	4.15	6.55	8.39	9.87
5	4.28	6.81	8.74	10.29
6	4.40	7.04	9.05	10.68
7	4.52	7.26	9.34	11.02
8	4.63	7.46	9.60	11.35
9	4.74	7.66	9.86	11.65
10	4.85	7.84	10.09	11.93

In the figure 4.7, when natural convection is dominated i.e., at  $Ri = 10.0$ , from streamline it observed that the velocity field forms a core of the vortex at  $Re = 50$ . The core of vortex increases with increases  $Re$  up to 150. In this folder at high  $Re = 200$ , the core of vortex squeezes and elongated along the length of the enclosure. It is also observed that the core of the vortex shifted right corner of the enclosure which indicating a sign of supremacy of natural convection in the enclosure. From streamline it is seen that the convective distortion of isothermal lines start to appear at  $Re = 50$  and at  $Ri = 10.0$ . It also seen that the isothermal lines turn back towards the right cold wall near the top of the enclosure and a thermal boundary layer is developed near the left vertical cold wall. At  $Re = 200$ , the lines of isotherms are almost parallel to horizontal line and condensed to side walls of the enclosure which is occurred due to the dominating influence of the convective current.

The effects of Reynolds number on average Nusselt number at the heat source is displayed as function of Richardson number at some particular Reynolds number in figure 4.8. It is observed that the average Nusselt number at the hot wall increases very sharply with increasing  $Ri$  for the higher values of Reynolds number  $Re$  ( $Re = 100, 150$  and  $200$ ), but is different for the lowest value of Reynolds number  $Re$  ( $Re = 50$ ). Also, maximum values of  $Nu$  is found for the highest value of  $Re$  ( $Re = 200$ ) at the pure forced convection region ( $Ri = 0.1$ ), at the pure mixed convection region ( $Ri = 1.0$ ) and free convection dominated region. In mixed convection dominated region, the heat transfer increases 51.34, 89.52, and 118.82% with increasing Reynolds number from  $Re = 50$  to 100, 150, and 200, respectively. Also in forced convection dominated region, the heat transfer increases 47.49, and 81.28 and 105.87% from  $Re = 50$  to 100, 150, and 200, respectively.

### 4.3 Effect of Prandtl number

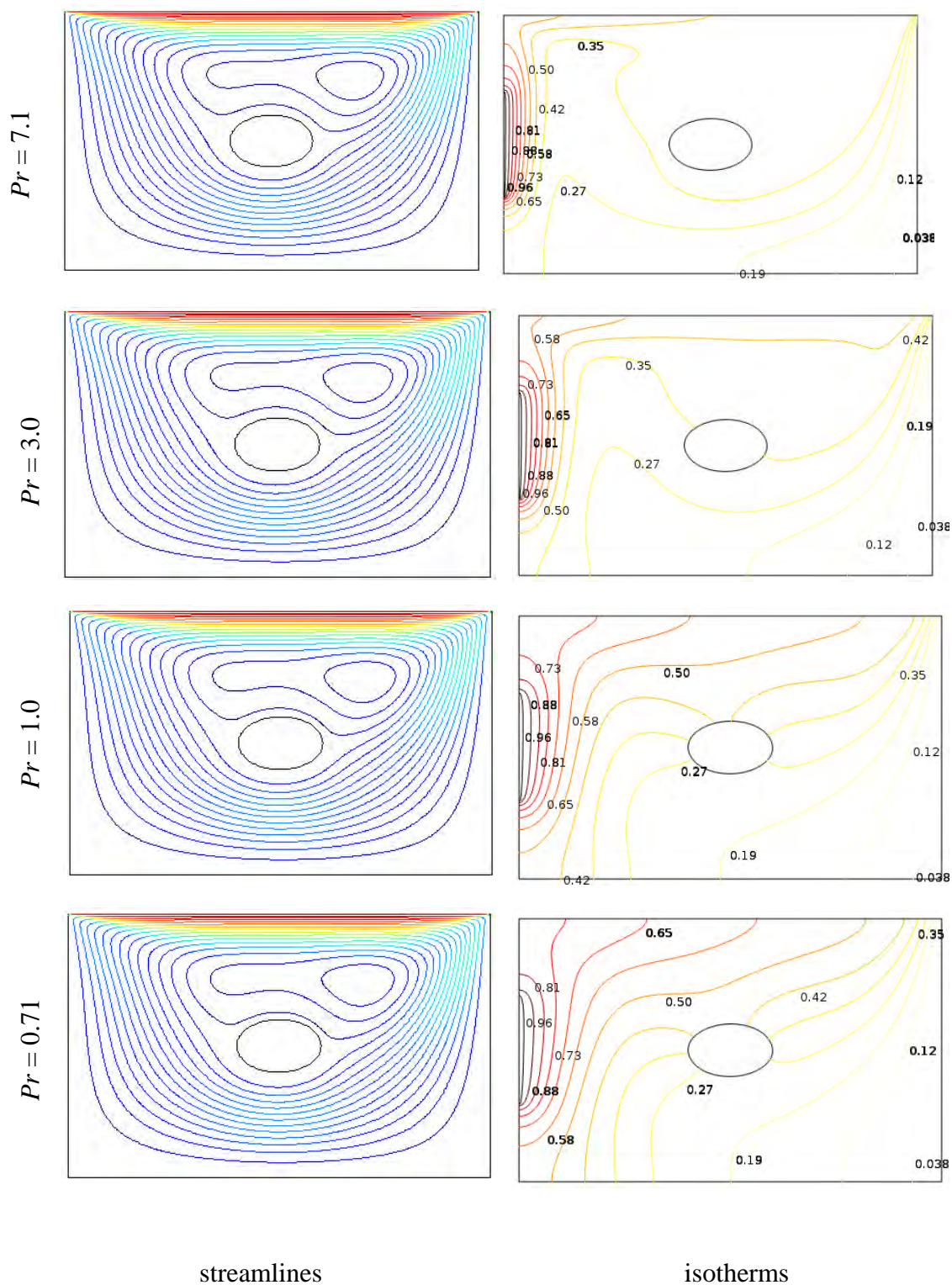
The effect of Prandtl number on the flow field as streamlines and on thermal characteristics as isotherms in the enclosure is shown in figure 4.9, 4.10, and 4.11 at different Richardson number  $Ri = 0.1$ ,  $Ri = 1.0$  and  $Ri = 10$  respectively while  $Re = 100$ , and  $Ha = 10$ . The streamlines for various  $Pr$  ( $Pr = 0.71, 1.0, 3.0$ , and  $7.1$ ) in the forced convection dominated region is shown in the left column of figure 4.9. Here the fluid flow is due to the shear induced force by the moving lid only. From this

figure, it can be seen that eyes of eddies are formed at  $Pr = 0.71$  and remains unchanged up to  $Pr = 7.1$ . From isotherms, it can be seen that thermal lines almost parallel to vertical walls at low  $Pr$  ( $Pr = 0.71$ ). On the other hand, the thermal lines are clustered to the side walls of the enclosure due to the severe temperature gradients in the vertical direction and number of isotherm lines decreases with increasing Prandtl number which means that, the convection heat transfer becomes more significant compared to the conduction one. Also it can be seen that, at  $Pr$  ( $Pr = 3.0$ ), a thinner thermal boundary layer is formed at the cold wall of the enclosure and thickness of the thermal boundary layer is increased at high Prandtl  $Pr$  ( $Pr = 7.1$ ).

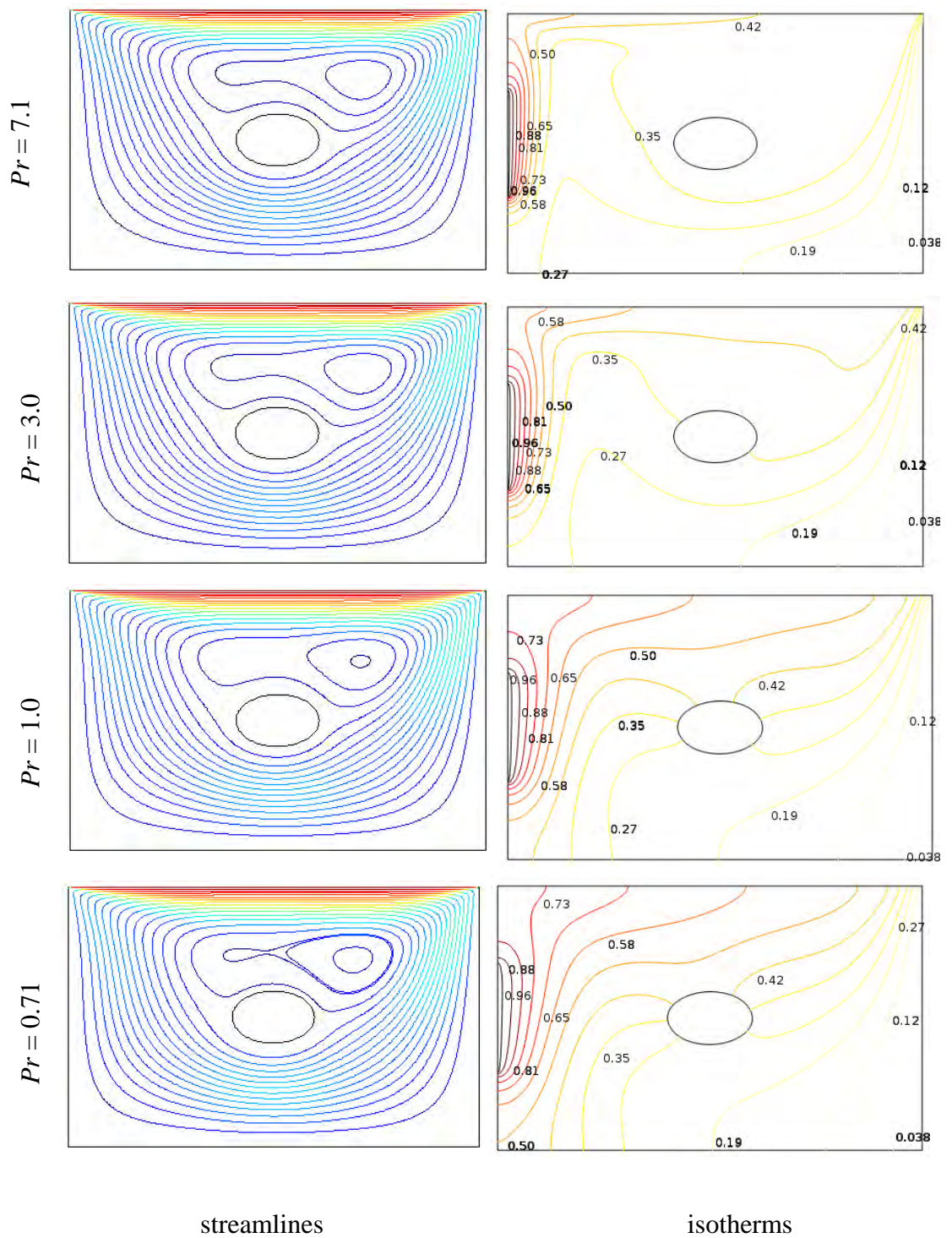
At  $Ri = 1$ , the balance between the shear and buoyancy effect is manifested in the formation of vortices inside the enclosure. From isotherm it is seen that the feature of the thermal lines similar to the feature of at  $Ri = 0.1$ .

From figure 4.11, it is observed that the fluid field forms two oval shaped eyes of eddies in the enclosure at  $Pr = 0.71$  with  $Ri = 10$ , which is the natural convection dominant region. At  $Pr = 1.0$ , the size of the oval shape decreased at the left half of enclosure and number of eyes of eddies are increased at the right half of enclosure. It is seen also that the oval shaped eyes of eddies merge into a unicellular vortex and shifted towards the left corner of the enclosure with increasing Prandtl number ( $Pr$ ). The physical meaning behind of the fact that the velocity field of the fluid are increased with increasing Prandtl number. From isotherms it is observed that the isothermal become more packed near the two side walls in the enclosure at higher Prandtl number. The bend in isothermal lines appears due to the high convective current inside the enclosure.

Figure 4.12 depicts the variation of average Nusselt number at the heated wall at varies values of Prandtl number ( $Pr$ ) and Richardson number ( $Ri$ ). From figure it is shown that the average Nusselt number ( $Nu$ ) increases slowly with increasing Prandtl number  $Pr$  ( $Pr = 0.71, 1.0$ ) which are generally considered as gas at different temperature. Such as 0.71 for air at 25°C and 1.0 for gas at 121°C. But average Nusselt number ( $Nu$ ) is quickly increases with higher values of Prandtl number  $Pr$  ( $Pr = 3.0, 7.1$ ) which are generally considered as water at different temperature. Such as 3.0 and 7.1 for water at 67°C and 20°C, respectively. At  $Ri = 10$ , heat transfer rate is maximum and average Nusselt number increases with increasing Prandtl number.

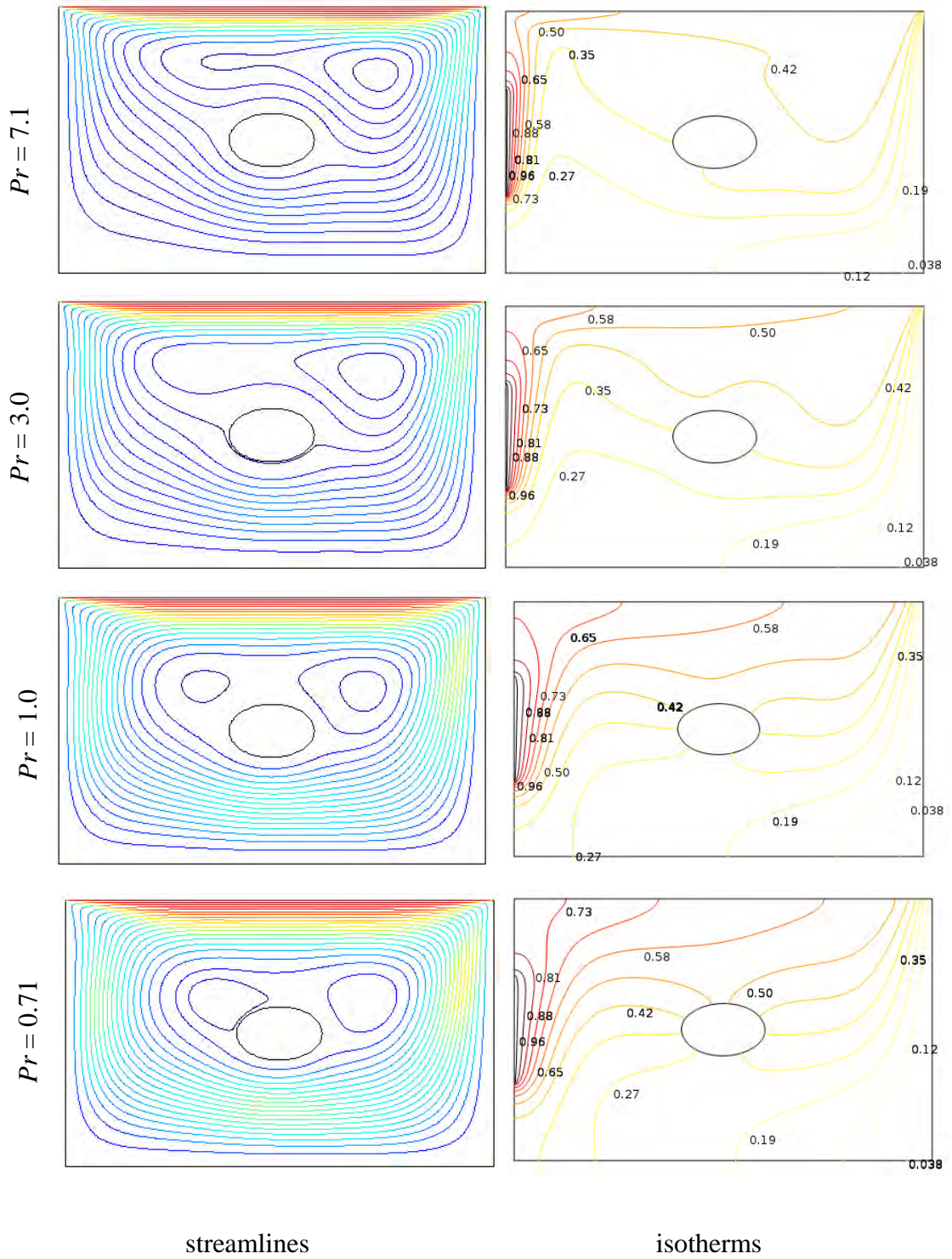


**Figure 4.9:** Effect of Prandtl number on streamlines and isotherms while  $Ri = 0.1$ ,  $Ha = 10$ ,  $Re = 100$ .

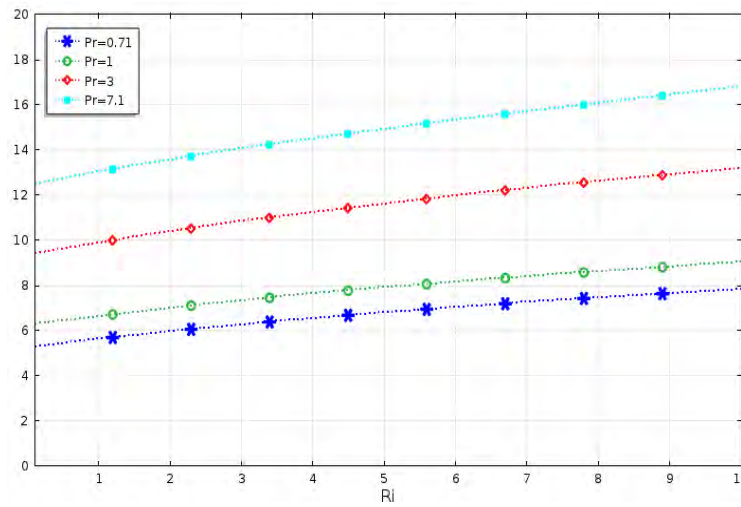


**Figure 4.10:** Effect of Prandtl number on streamlines and isotherms while  $Ri = 1.0$ ,  $Ha = 10$ ,  $Re = 100$ .





**Figure 4.11:** Effect of Prandtl number on streamlines and isotherms while  $Ri = 10$ ,  $Ha = 10$ ,  $Re = 100$ .



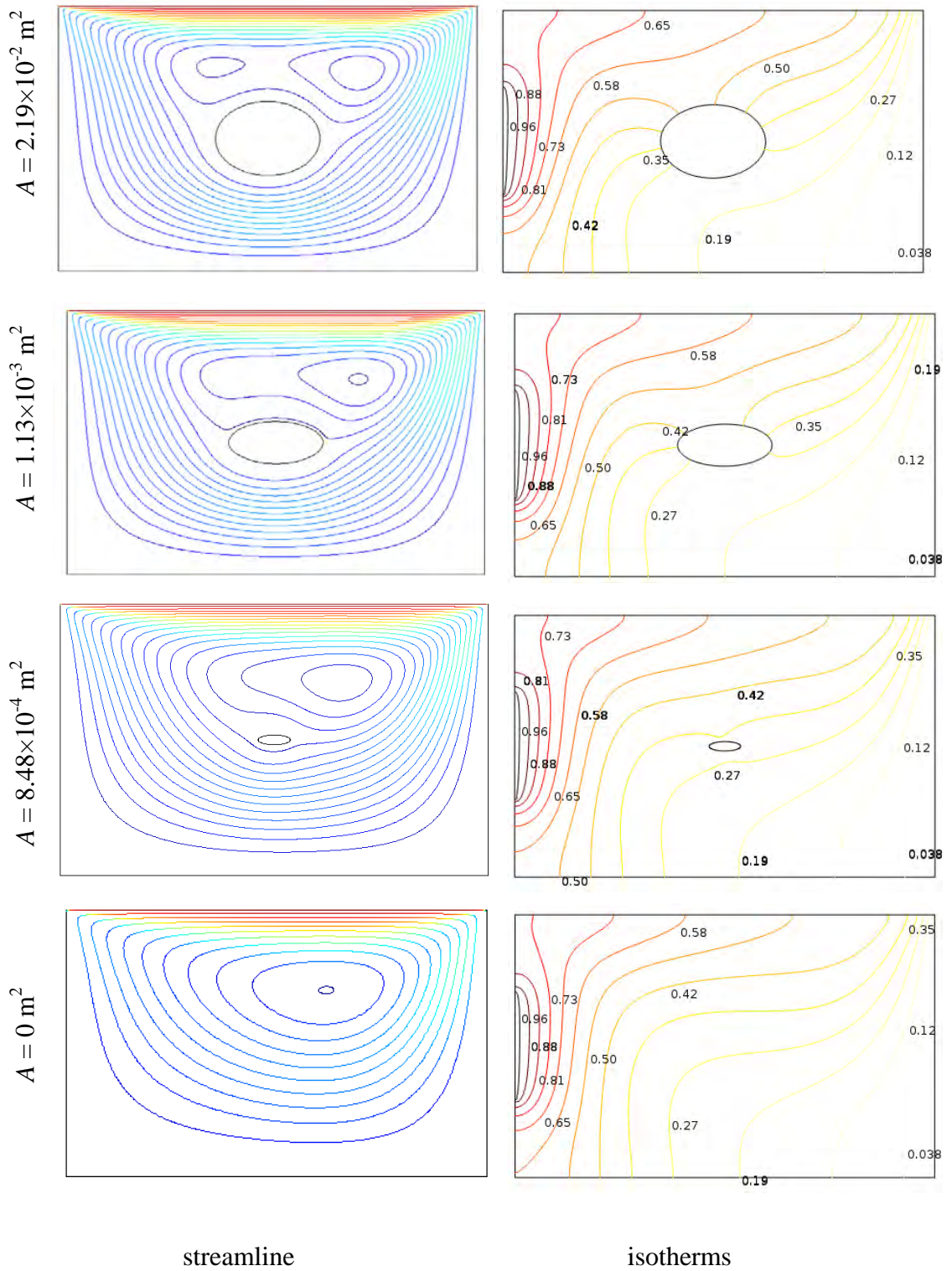
**Figure 4.12:** Effect of Prandtl Number  $Pr$  on average Nusselt number, while  $Re = 100$ ,  $Ha = 10$ .

**Table 4.3:** Variation of average Nusselt number with Prandtl number for different Richardson number

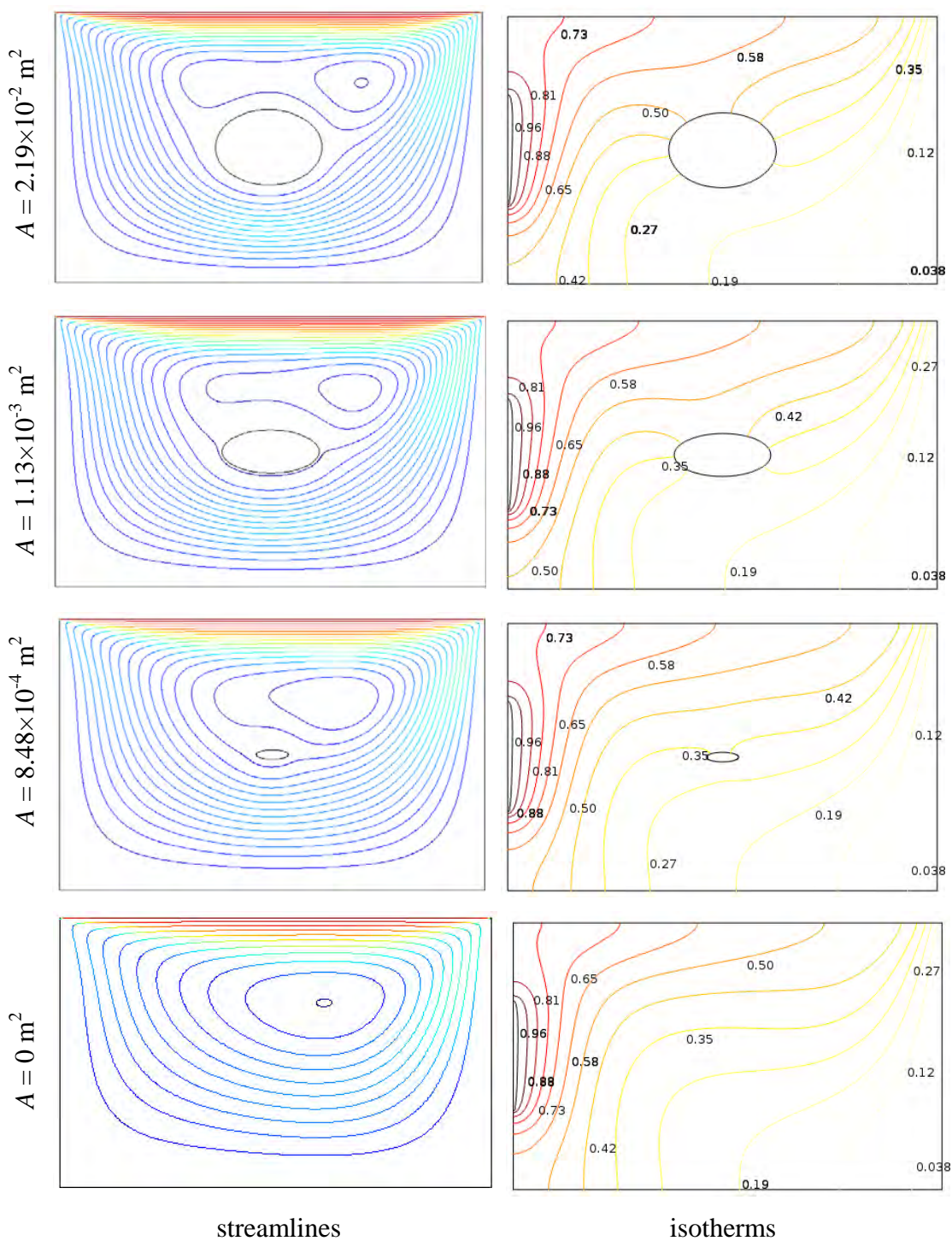
$Ri$	$Nu_{av}$			
	$Pr = 0.71$	$Pr = 1$	$Pr = 3$	$Pr = 7.1$
0.1	5.28	6.28	9.40	12.50
1	5.63	6.65	9.90	13.04
2	5.97	7.01	10.39	13.58
3	6.28	7.34	10.84	14.06
4	6.55	7.64	11.25	14.50
5	6.81	7.91	11.63	14.92
6	7.04	8.17	11.98	15.32
7	7.26	8.40	12.31	15.70
8	7.47	8.63	12.62	16.08
9	7.66	8.84	12.92	16.45
10	7.84	9.03	13.19	16.81

#### 4.4 Effect of area of block

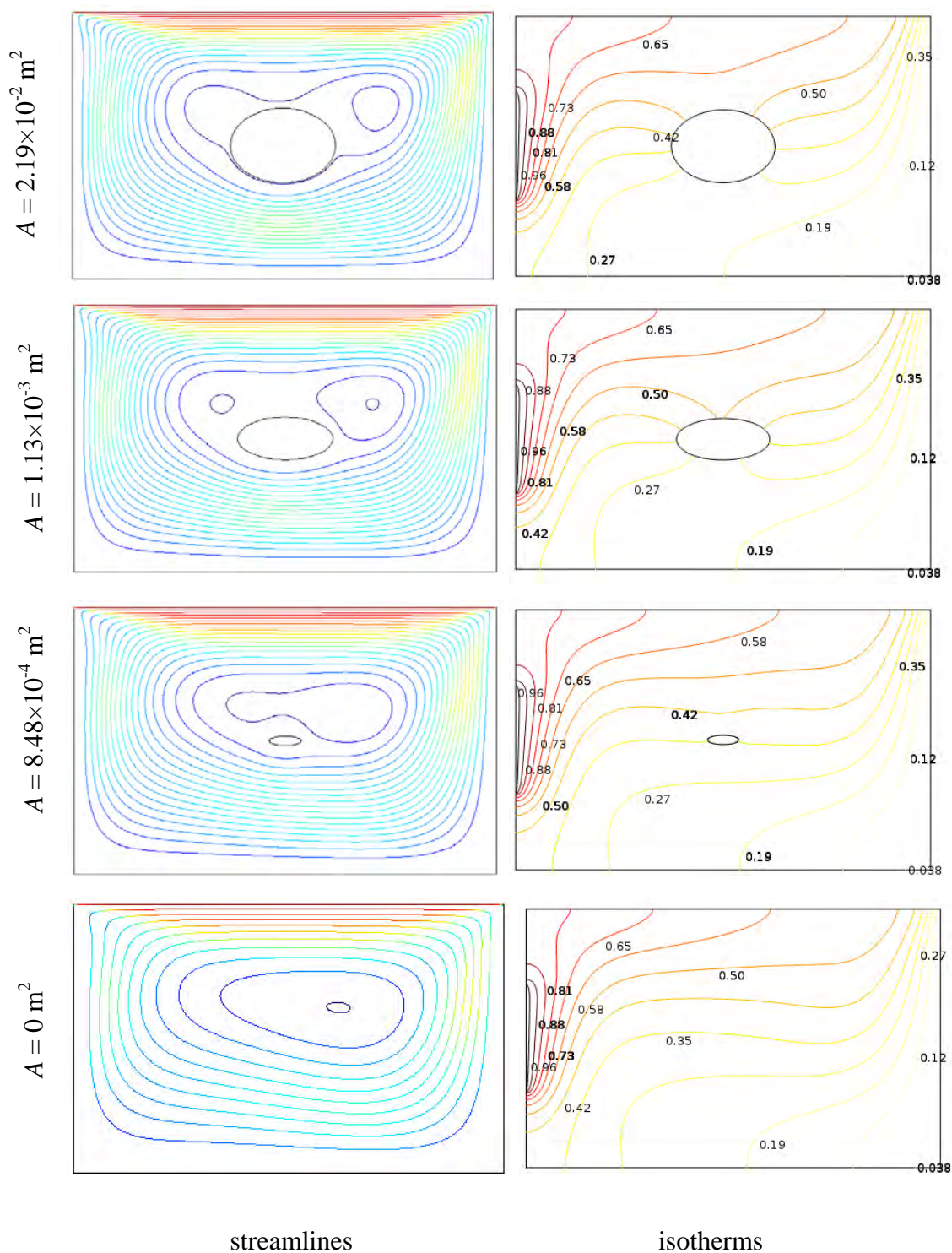
The effect of area of elliptical block (placed at center of the enclosure ) on the flow field as streamline and thermal field as isotherms in a rectangular enclosure operating at different three values of  $Ri = 0.1, 1,$  and  $10$  are presented in the figure 4.13, 4.14 and 4.15 respectively while  $Re = 100, Pr = 0.71$  and  $Ha = 10$  are kept fixed. At  $Ri = 0.1$ , when force convection dominated, the recirculation flow in the enclosure mostly generated only by the moving lid at  $A = 0 \text{ m}^2$ , which presented in figure 4.13. The recirculation flow rotates in clockwise direction, which is expected since the lid is moving left to right. At higher values of  $A$  ( $A = 8.48 \times 10^{-4}, 1.13 \times 10^{-3}$  and  $2.19 \times 10^{-2} \text{ m}^2$ ), the flow patterns inside the cavity remain unchanged except the shape and position of core of the circulatory flow. At  $A = 2.19 \times 10^{-2} \text{ m}^2$ , the core of the recirculation cell increased and elongated to the side walls due to large size of the block which oppose the velocity of the fluid. The corresponding effect of isotherms is presented at right column of figure 4.13. From isotherms it can be seen that at  $A = 0 \text{ m}^2$ , the thermal lines near the hot wall parallel to the heated surface and parabolic shape isotherms are seen in middle of the enclosure, which is similar to forced convection and conduction like distribution. At higher values of  $A$ , there is no significant change except middle position of the enclosure. Next at  $Ri = 1$ , there is no change at low values of  $A$  ( $A = 8.48 \times 10^{-4} \text{ m}^2$ ) but at  $A = 8.48 \times 10^{-4} \text{ m}^2$ , an eye of eddies is produced. The length of eye of eddies is increased with increasing area of block and shifted upward side of the enclosure due to both lid and shear driven force in the enclosure. Furthermore, similar trend is observed in the isotherms for different values of  $A$  at  $Ri = 1.0$ , which is due to mixed convection flow in the enclosure. At  $A = 0 \text{ m}^2$ , elliptical shaped isothermal lines are developed at the right top corner in the enclosure. In addition, the convective distortion in the isothermal lines near the right top corner in the enclosure gradually decreases with increasing the value of  $A$ . This behavior is very logical because the large elliptical area reduces the buoyancy effects.



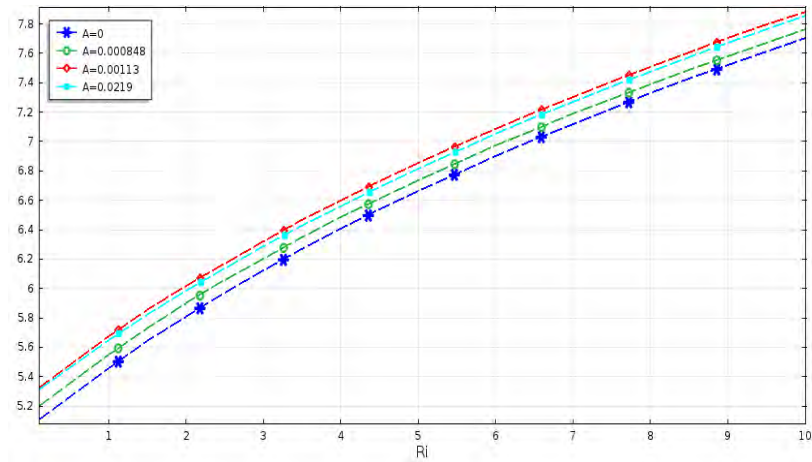
**Figure 4.13:** Effect of streamlines and isotherms on different elliptical area at Richardson number  $Ri = 0.1$  while  $Re = 100$ ,  $Ha = 10.0$  and  $Pr = 0.71$ .



**Figure 4.14:** Effect of different elliptical area on streamlines and isotherms while  $Ri = 1$ ,  $Ha = 10$ ,  $Re = 100$  and  $Pr = 0.71$ .



**Figure 4.15:** Effect of different Elliptical area on streamlines and isotherms while  $Ri = 10$ ,  $Ha = 10$ ,  $Re = 100$ .and  $Pr = 0.71$



**Figure 4.16:** Effect of area of block on average Nusselt number, while  $Re = 100$ ,  $Pr = 0.71$  and  $Ha = 10$ .

**Table 4.4:** Variation of average Nusselt number with area of block for different Richardson number

$Ri$	$Nu_{av}$			
	$A = 0 \text{ m}^2$	$A = 8.48 \times 10^{-4} \text{ m}^2$	$A = 1.13 \times 10^{-3} \text{ m}^2$	$A = 2.19 \times 10^{-2} \text{ m}^2$
0.1	5.10	5.20	5.32	5.31
1	5.45	5.55	5.67	5.65
2	5.81	5.90	6.01	5.98
3	6.12	6.20	6.32	6.28
4	6.41	6.48	6.60	6.56
5	6.66	6.73	6.85	6.81
6	6.90	6.97	7.08	7.05
7	7.11	7.18	7.30	7.27
8	7.32	7.39	7.51	7.47
9	7.52	7.58	7.70	7.67
10	7.70	7.76	7.88	7.85

Further at  $Ri = 10$  which is buoyancy dominated region regime, the recirculation cells of the vortices are formed and occupy most of the part of the enclosure at  $A = 0 \text{ m}^2$  which is shown in figure 4.15. At  $A = 1.13 \times 10^{-3} \text{ m}^2$ , two minor core of the recirculation cells are formed. This is because convective current is increased with increasing the value of  $A$ . But at highest value of  $A$ , the core of vortices elongated along the horizontal in the half top of the enclosure because large size of block reduces the space of the enclosure. Consequently the velocity field of the enclosure is reduced. From isotherms, it can be seen that at absence of area of block, the thermal lines are almost parallel to the horizontal wall which means that the conduction heat transfer is less than convection heat transfer.

The variation of average Nusselt number ( $Nu$ ) at the heated surface against  $Ri$  at various values of  $A$  is shown in figure 4.16. From these figures it is observed that the average Nusselt number ( $Nu$ ) monotonically increases with increasing  $Ri$ . It is also seen that the average Nusselt number ( $Nu$ ) increases up to  $A = 1.13 \times 10^{-3} \text{ m}^2$ . But at large value of  $A$  the average Nusselt number ( $Nu$ ) decreases. That means the heat transfer rate increases up to certain area of block and then decreased with increasing the area of the block. This is because large area of the block opposes the velocity of the flow and reduces the temperature gradients. Finally, the quantitative values of  $Nu$  at different values of area of block are listed in the Table 4.4



# Chapter 5

## Conclusions

---

Magnetohydrodynamic mixed convection in obstructed lid-driven rectangular enclosure has been investigated numerically. The results are presented for streamlines and isotherms as well as heat transfer rate both in tabular and graphical form. Comparisons with the beforehand published work are done and found to be in excellent agreement. The influences of Hartmann number, Richardson number, Reynolds number, Prandtl number and area of the block have been reported. The various ideas and results have been discussed in individual detail at the relevant chapter of the thesis. In the present chapter an attempt is made to summaries the concepts presented and results obtained in the work reported already. A section on the scope of further work on associated fields of investigation is also included.

### 5.1 Summary of the Major Outcomes

MHD mixed convection flow in a rectangular lid-driven enclosure along with an adiabatic elliptical block has been investigated numerically. A magnetic field has been introduced parallel to the horizontal direction. From the investigation the following conclusions have been drawn:

- (i) Magnetic field affects the flow and temperature fields and it delays the heat transfer from the heated surface. However, maximum average Nusselt number ( $Nu$ ) are obtained at the highest value of Richardson number ( $Ri = 10$ ) i.e in natural convection dominated region.
- (ii) Reynolds number ( $Re$ ) has significant effects on the flow field at the pure mixed convection and free convection dominated region. Also  $Re$  has significant effect on temperature field at the three convective regimes. However, the average Nusselt number with  $Ri$  increases with increasing  $Re$ . Moreover at high Reynolds number ( $Re = 200$ ), the heat transfer rate is maximum in the natural convective region.
- (iii) Prandtl number ( $Pr$ ) does not have significant contribution on the flow field at the forced convection and mixed convection dominated region, whereas there are remarkable changes in the thermal field as  $Pr$  changes for a particular  $Ri$ .

The average Nusselt number ( $Nu$ ) monotonically increases at lowest  $Pr$ . But at higher values of  $Pr$ , the average Nusselt number ( $Nu$ ) increases very quickly. In addition the values of  $Nu$  is always superior for the large value of  $Pr$ .

- (iv) Area of elliptical block has significant influence on the flow in the natural convection dominated region and on the thermal fields. The average Nusselt number ( $Nu$ ) increases at certain area of elliptical block. But at highest area of elliptical block ( $A = 2.19 \times 10^{-2} \text{ m}^2$ ), the average Nusselt number decreases. However, higher average Nusselt number is always observed for the largest value of  $Ri$ .
- (v) Moreover, noticeably different flow and heat transfer behavior are observed among the three different flow regimes.

## 5.2 Further Works

The following recommendation can be put forward for the further works on this present research as:

- ❖ In the future, the study can be extended by incorporating different physics like internal heat generation / absorption, capillary effects.
- ❖ Double lid-driven MHD mixed convection can be performed through including the governing equation of concentration conservation.
- ❖ Investigation can be analyzed by using magnetic fluid instead of electrically conducting fluid within the porous medium.
- ❖ Analysis can be continued by changing the boundary conditions of the enclosure's walls.
- ❖ The study can be extended for turbulent flow using different fluids, different thermal boundary conditions such as constant heat flux and unsteady flow.
- ❖ Only two-dimensional fluid flow and heat transfer has been performed in this thesis. So this deliberation may be extended to three-dimensional analyses to investigate the effects of parameters on flow fields and heat transfer in enclosure.

## References

---

- [1] Chowdhury, K., and Alim, M.A., “Analysis of MHD mixed convection flow within a square enclosure containing a triangular obstacle”, *American Journal of Applied Mathematics*, vol. 3, pp. 288-296, 2015.
- [2] Khudheyr, A.F., “MHD mixed convection in double lid-driven differentially heated trapezoidal cavity”, *International Journal of Application or Innovation in Engineering and Management*, vol. 4, pp. 100-107, 2015.
- [3] Bakar, N.A., Roslan, R., Karimipour, A., and Hashim, I., “Mixed convection in a lid-driven cavity with inclined magnetic field”, *Sains Malaysiana*, vol. 48, pp. 451-471, 2019.
- [4] Parvin, S., and Nasrin, R., “Analysis of the flow and heat transfer characteristics for MHD free convection in an enclosure with a heated obstacle”, *Nonlinear Analysis: Modeling and Control*, vol. 16, pp. 89-99, 2011.
- [5] Saha, L.K., Somadder, M.C., and Salah Uddin, K.M., “Mixed convection heat transfer in a lid driven cavity with wavy bottom surface”, *American Journal of Applied Mathematics*, vol 1, pp. 92-101, 2013.
- [6] Ismael, M.A., Pop, A., and Chamkha, A.J., “Mixed convection in a lid-driven square cavity with partial slip”, *International Journal of Thermal Sciences*, vol. 82, pp. 47-61, 2014.
- [7] Sumon, S., Hasan, M.N., Saha, G., and Islam, M.Q., “Effect of inclination angle on mixed convection in a lid-driven square enclosure with internal heat generation or absorption”, *International Conference on Mechanical, Industrial and Energy Engineering*, MIE10-149-6, 2010.
- [8] Malleswaran, A., and Sivasankaran, S., “A numerical simulation on MHD mixed convection in a lid-driven cavity with corner heaters”, *Journal of Applied Fluid Mechanics*, vol. 9, pp. 311-319, 2016.
- [9] Nasrin, R., “Mixed magnetoconvection in a lid driven cavity with a

- sinusoidal wavy wall and a central heat conducting body”, *Journal of Naval Architecture and Marine Engineering*, vol. 7, pp. 13-24, 2010.
- [10] Afolabi, S.I., Ojo, A.O., Oluleye, M.A., and Ojo, A.A., “Convective heat transfer in a square cavity with a heat-generating body at different aspect ratios”, *International Journal of Engineering and Technology*, vol. 8, pp. 555-562, 2019.
- [11] Keshtkar, M.M., and Ghazanfari, M., “Numerical investigation of fluid flow and heat transfer inside a 2D enclosure with three hot obstacles on the ramp under the influence of a magnetic field”, *Engineering Technology and Applied Science Research*, vol. 7, pp. 1647-1657, 2017.
- [12] Rahman, M.M., Oztop, H.F., Rahim, N.A., Saidur, R., Al-Salem, K., Amin, N., Mamun M.A.H., and Asan, A., “Computational analysis of mixed convection in a channel with a cavity heated from different sides”, *International Communication in Heat and Mass Transfer*, vol. 39, pp. 78-84, 2012.
- [13] Billah, M.M., Rahman, M.M., Sharif, U.M., Rahim, N.A., Saidur, R., and Hassanuzzaman, M., “Numerical analysis of fluid flow due to mixed convection in a lid-driven cavity having a heated circular hollow cylinder”, *International Communication in Heat and Mass Transfer*, vol. 38, pp. 1098-1103, 2011.
- [14] Sivanandam, S., Malleswaran, A., Lee, J., and Sundar, P., “Hydro-magnetic combined convection in a lid-driven cavity with sinusoidal boundary conditions on both side walls”, *International Journal of Heat and Mass Transfer*, vol. 54, pp. 512-525, 2011.
- [15] Oztop, H.F., Al-Salim, K., and Pop, L., “MHD mixed convection in a lid-driven cavity with corner heater”, *International Journal of Heat and Mass Transfer*, vol. 54, pp. 3494-3504, 2011.
- [16] Basak, T., Roy, S., Sharma, P.K., and Pop, I., “Analysis of mixed convection flows within a square cavity with linearly heated side wall”, *International*

- Journal of Heat and Mass Transfer, vol. 52, pp. 2224-2242, 2009.
- [17] Ching, Y.C., Oztop, H.F., Rahman, M.M., Islam, M.R., and Ahsan, A., “Finite element simulation of mixed convection heat and mass transfer in a right triangular enclosure”, *International Communication in Heat and Mass Transfer*, vol. 39, pp. 689-696, 2012.
- [18] Khanafer, K., and Aithel, S.M., “Laminar mixed convection flow and heat transfer characteristics in a lid-driven cavity with a circular cylinder”, *International Communication in Heat and Mass Transfer*, vol. 66, pp. 200-209, 2013.
- [19] Omary, R., “CFD simulations of lid-driven cavity flow at moderate Reynolds number”, *European Scientific Journal*, vol. 9, pp. 22-35, 2013.
- [20] Biswas, N., and Mahapatra, P.S., “Enhanced thermal energy transport using adiabatic block inside lid-driven cavity”, *International Journal of Heat and Mass Transfer*, vol. 100, pp. 407-427, 2016.
- [21] Guo, G., and Sharif, M.A.R., “Mixed convection in rectangular cavities at various aspect ratios with moving isothermal sidewalls and constant flux heat source on the bottom wall”, *International Journal of Thermal sciences*, vol. 43, pp. 465-475, 2004.
- [22] Mousa, M.M., “Modeling of laminar buoyancy convection in a square cavity containing an obstacle”, *Mathematics Subject Classification*, 65M60, 76D05, 80A20.
- [23] Rahman M.M., and Alim, M.A., “MHD mixed convection flow in a lid-driven square enclosure including a heat conducting horizontal circular cylinder with joule heating”, *Nonlinear Analysis: Modeling and Control*, vol. 115, pp. 199-211, 2010.
- [24] Abraham, J., and Varghese, J., “Mixed convection in a differentially heated square cavity with moving lids”, *International Journal of Research and Technology*, vol. 4, pp. 602-607, 2015.
- [25] Kosti, S., and Rathore, V.S., “Numerical study of lid-driven cavity at

- different Reynolds number”, Trends in Mechanical Engineering and Technology, Vol. 5, pp. 1-5, 2015.
- [26] Zheng, G.F., Ha, M.Y., Yoon, H.S., and Park, Y.G., “A numerical study on mixed convection in a lid-driven cavity with a circular cylinder”, Journal of Mechanical Science and Technology, vol. 27, pp. 273-286, 2013.
- [27] Hussein, A.K., and Hussain, S.H., “Characteristics of magnetohydrodynamic mixed convection in a parallel motion two-sided lid-driven differentially heated parallelogrammic cavity with various skew angles”, Journal of Thermal Engineering, vol. 1, pp. 221-235, 2015.
- [28] YadollahiFarsani, R., and Ghasemi, B., “Magnetohydrodynamic mixed convective flow in a cavity”, International Journal of Mechanical and Mechatronics Engineering, vol. 15, pp. 2328-2331, 2011.
- [29] Anderson, J.D., “Computational fluid dynamics”, International Ed., McGraw-Hill, 1995.
- [30] Cengel, Y.A., “Heat and mass transfer”, Third Ed., Tata McGraw-Hill, 2007.
- [31] Chung, T.J., “Computational fluid dynamics”, First Ed., Cambridge University Press, 2002.
- [32] Dechaumphai, P., “Finite Element Method in Engineering”, second Ed., Chulalongkorn University Press, Bangkok, 1999.
- [33] Patankar, S.V., “Numerical heat transfer and fluid flow”, Second Ed., Washington, D. C. Homisphere, 1980.
- [34] Shercliff, J.A., “A Textbook of Magnetohydrodynamics, First Ed., Pergamon” Press, UK, 1965.
- [35] Zienkiewicz, O.C., and Taylor, R.L., “The finite element method”, Fourth Ed., McGraw-Hill, 1991.
- [36] Ferziger, J.H., and Perić, M., “Computational methods for fluid dynamics”, Second Ed., Springer Verlag, Berlin Heidelberg, 1997

- [37] Fletcher, C.A.J., “Computational techniques for fluid dynamics 1”, Second Ed., Springer Verlag, Berlin Hedelberg, 1991.
- [38] Reddy, J.N., and Gartling, D.K., “The Finite Element Method in Heat Transfer and Fluid Dynamics”, CRC Press, Inc., Boca Raton, Florida, 1994.
- [39] Kakac, S., And Yener, Y., “Convective Heat Transfer”, Second Ed., CRC Press, Taylor and Francis Group, 1994.